



**HAL**  
open science

## Exploration of a European-centered strawberry diversity panel provides markers and candidate genes for the control of fruit quality traits

Alexandre Prohaska, Pol Rey-Serra, Johann J. Petit, Aurélie Petit, Justine Perrotte, Christophe Rothan, Béatrice Denoyes

### ► To cite this version:

Alexandre Prohaska, Pol Rey-Serra, Johann J. Petit, Aurélie Petit, Justine Perrotte, et al.. Exploration of a European-centered strawberry diversity panel provides markers and candidate genes for the control of fruit quality traits. *Horticulture research*, 2024, 10.1093/hr/uhae137/7672963 . hal-04612454

**HAL Id: hal-04612454**

**<https://hal.inrae.fr/hal-04612454>**

Submitted on 14 Jun 2024

**HAL** is a multi-disciplinary open access archive for the deposit and dissemination of scientific research documents, whether they are published or not. The documents may come from teaching and research institutions in France or abroad, or from public or private research centers.

L'archive ouverte pluridisciplinaire **HAL**, est destinée au dépôt et à la diffusion de documents scientifiques de niveau recherche, publiés ou non, émanant des établissements d'enseignement et de recherche français ou étrangers, des laboratoires publics ou privés.



Distributed under a Creative Commons Attribution 4.0 International License

# 1 Article Title

2 **Exploration of a European-centered strawberry diversity panel provides markers and candidate genes for**  
3 **the control of fruit quality traits**

4  
5 **Running title:** GWAS of strawberry quality traits and candidate genes

6  
7 Alexandre Prohaska<sup>1,2</sup>, Pol Rey-Serra<sup>1</sup>, Johann Petit<sup>1</sup>, Aurélie Petit<sup>2</sup>, Justine Perrotte<sup>2</sup>, Christophe Rothan<sup>1\*</sup>,  
8 Béatrice Denoyes<sup>1\*</sup>

9 <sup>1</sup> Univ. Bordeaux, INRAE, UMR BFP, F-33140, Villenave d'Ornon, France.

10 <sup>2</sup> Invenio, MIN de Brienne, 110 quai de Paludate, 33000 Bordeaux, France

11  
12 \* Corresponding authors:

13 **Béatrice Denoyes** <https://orcid.org/0000-0002-0369-9609>

14 Email: [beatrice.denoyes@inrae.fr](mailto:beatrice.denoyes@inrae.fr); Phone: +335 57 12 24 60

15 UMR BFP – INRAE, 71 avenue Edouard Bourlaux, 33140 Villenave d'Ornon, France

16 **Christophe Rothan** <https://orcid.org/0000-0002-6831-2823>

17 Email: [christophe.rothan@inrae.fr](mailto:christophe.rothan@inrae.fr); Phone: +335 57 12 24 60 ;

18 UMR BFP – INRAE, 71 avenue Edouard Bourlaux, 33140 Villenave d'Ornon, France

19  
20 Alexandre Prohaska: [alexandre.prohaska@gmail.com](mailto:alexandre.prohaska@gmail.com); <https://orcid.org/0009-0004-0395-7470>

21 Pol Rey-Serra: [pol.rey-serra@inrae.fr](mailto:pol.rey-serra@inrae.fr); <https://orcid.org/0000-0002-3685-2470>

22 Johann Petit: [johann.petit@inrae.fr](mailto:johann.petit@inrae.fr); <https://orcid.org/0000-0002-6746-1755>

23 Aurélie Petit: [a.petit@invenio-fl.fr](mailto:a.petit@invenio-fl.fr); <https://orcid.org/0000-0003-1577-9072>

24 Justine Perrotte: [j.perrotte@invenio-fl.fr](mailto:j.perrotte@invenio-fl.fr)

25 Christophe Rothan: [christophe.rothan@inrae.fr](mailto:christophe.rothan@inrae.fr); <https://orcid.org/0000-0002-6831-2823>

26 Béatrice Denoyes: [beatrice.denoyes@inrae.fr](mailto:beatrice.denoyes@inrae.fr); <https://orcid.org/0000-0002-0369-9609>

27  
28  
29 © The Author(s) 2024. Published by Oxford University Press. This is an Open Access article distributed

30 under the terms of the Creative Commons Attribution License

31 <https://creativecommons.org/licenses/by/4.0/>, which permits unrestricted reuse, distribution, and

32 reproduction in any medium, provided the original work is properly cited.

33

## 34 Abstract

35 Fruit quality traits are major breeding targets in cultivated strawberry (*Fragaria × ananassa*). Taking into  
36 account the requirements of both growers and consumers when selecting high quality cultivars is a real  
37 challenge. Here, we used a diversity panel enriched with unique European accessions and the 50K FanaSNP  
38 array to highlight the evolution of strawberry diversity over the past 160 years, investigate the molecular  
39 basis of 12 major fruit quality traits by Genome-Wide Association Studies (GWAS), and provide genetic  
40 markers for breeding. Results show that considerable improvements of key breeding targets including fruit  
41 weight, firmness, composition and appearance occurred simultaneously in European and American  
42 cultivars. Despite the high genetic diversity of our panel, we observed a drop in nucleotide diversity in  
43 certain chromosomal regions, revealing the impact of selection. GWAS identified 71 associations with 11  
44 quality traits and, while validating known associations (firmness, sugar), highlighted the predominance of  
45 new QTL, demonstrating the value of using untapped genetic resources. Three of the six selective sweeps  
46 detected are related to glossiness or skin resistance, two little-studied traits important for fruit  
47 attractiveness and, potentially, postharvest shelf-life. Moreover, major QTL for firmness, glossiness, skin  
48 resistance and susceptibility to bruising are found within a low diversity region of chromosome 3D.  
49 Stringent search for candidate genes underlying QTL uncovered strong candidates for fruit color, firmness,  
50 sugar and acid composition, glossiness and skin resistance. Overall, our study provides a potential avenue  
51 for extending shelf-life without compromising flavor and color as well as the genetic markers needed to  
52 achieve this goal.

53

54 **Keywords:** *Fragaria × ananassa*, strawberry, diversity, fruit quality, GWAS, candidate genes

55

56

## 57 Introduction

58

59 Cultivated strawberry (*Fragaria × ananassa*), the most widely consumed small fruit worldwide, results from  
60 spontaneous hybridization in botanical gardens in France in the 18<sup>th</sup> century between two octoploid ( $2n =$   
61  $8x = 56$ ) species (*F. chiloensis* and *F. virginiana*) imported from the New World<sup>1</sup>. Since then, cultivated  
62 strawberry has been continuously improved through the introgression of alleles from wild progenitors  
63 creating an admixed population of interspecific hybrid lineages<sup>2,3,4</sup>. Recurrent hybridization contributed to  
64 maintain genetic diversity in the domesticated populations<sup>4</sup>. However, lower genetic diversity and  
65 heterozygosity can be observed in highly structured populations, which nevertheless show considerably  
66 improved yield, fruit weight and firmness<sup>5</sup>. Current efforts, triggered by consumer demand for sweet and  
67 highly-flavored strawberries<sup>6,7</sup>, are aimed at improving the sensory and nutritional quality traits of the fruit  
68 such as color<sup>8</sup> and flavor<sup>9</sup>. Another area for improvement is the extension of the storage period and the  
69 reduction of post-harvest rot, both of which are linked to fruit firmness<sup>7</sup> and little-explored fruit surface  
70 properties<sup>10</sup>. Several fruit quality traits can be easily manipulated using advanced technology, such as  
71 genome editing which has successfully been applied to create new alleles modifying various traits including  
72 fruit color, sweetness and aroma<sup>7,11</sup>. Other complex (e.g. fruit size) and/or little-studied (e.g. fruit  
73 glossiness) traits first require elucidation of their genetic architecture. Until recently, following initial  
74 studies<sup>12,13</sup>, the dissection of the genetic control of complex fruit quality traits in *F. × ananassa* has mainly  
75 been achieved by mapping Quantitative Trait Locus (QTL) on genetic linkage maps of bi-parental<sup>14,15,16</sup> or  
76 multi-parental<sup>17</sup> populations. Causal genetic variants have been identified for several QTL, leading to the  
77 design of genetic markers for marker-assisted selection (MAS) of strawberry varieties with, for example,  
78 improved fruit color<sup>8,18</sup> and better aroma<sup>9</sup>.

79

80 Complexity of the allo-octoploid genome of *F. × ananassa*, where up to eight homeo-allelic forms of the  
81 same gene can be found<sup>19</sup>, has until recently hampered the mapping of QTLs on a given chromosome.  
82 Whole genome sequencing of *F. × ananassa*<sup>1</sup> and, more recently, its progenitors<sup>20</sup>, showed that the four  
83 subgenomes of *F. × ananassa* are derived from the diploids *F. vesca* and *F. iinumae* and from two extinct  
84 species related to *F. iinumae*<sup>20,21</sup>. Genome sequence further enabled the design of a single nucleotide  
85 polymorphism (SNP) 50K array with selected chromosome-specific SNPs<sup>22</sup> allowing the high-resolution  
86 mapping of QTLs. A recent breakthrough has been the completion of haplotype-resolved genomes for five  
87 genotypes of *F. × ananassa*<sup>9,23,24,25,26</sup>. These developments make it possible to exploit strawberry diversity  
88 through genome wide association studies (GWAS), which scans the genome for significant associations  
89 between genetic markers and the trait studied<sup>2</sup>. It thus can help unveil beneficial alleles through the  
90 exploration and characterization of strawberry genetic resources, which display a wide genetic and  
91 phenotypic diversity<sup>4,27,28,29</sup>. So far, GWAS has been done on collections mostly centered on North American

92 strawberry populations<sup>4,29</sup>, which enabled the discovery of major QTLs controlling fruit weight, firmness,  
93 sweetness and aroma<sup>4,9,29,30,31</sup>. It would certainly benefit from the exploration of other less well-  
94 characterized germplasm found in Europe<sup>32</sup>, a historically active strawberry breeding center<sup>6</sup>.

95

96 In this study, we explored by GWAS the genetic architecture of fruit quality in *F. × ananassa*. To this end, we  
97 used the unexploited genetic diversity found in traditional and modern European varieties, in comparison  
98 with the better described diversity of North American varieties and some Asian genotypes. Our results are  
99 consistent with recent insights into the evolution of modern strawberry varieties and detected major QTL  
100 recently described, for fruit firmness for example. Moreover, we detected new QTL for most of the 12 fruit  
101 quality traits studied and the underlying candidate genes (CG). An example of this are the QTL and strong  
102 CG for the little-explored glossy trait, which underpins the shiny appearance of all modern strawberry  
103 varieties and was found to co-localize with a skin resistance trait. Our results therefore highlight the  
104 richness of European collections as a source of genetic diversity for strawberry breeding.

105

## 106 Results

107

### 108 Population structure and genetic diversity of the diversity panel of cultivated strawberry

109 We analyzed a germplasm diversity panel comprising 223 accessions of cultivated strawberries (*F. ×*  
110 *ananassa*) available at Invenio (South-West France) (Table S1). Unlike the main diversity panels studied to  
111 date, where the bulk of the panel was constituted by North American accessions<sup>4,28</sup>, our panel was mostly  
112 composed of European accessions from several countries, with French cultivars being by far the most  
113 represented (96 accessions). In addition, the panel comprised representative cultivars from North America  
114 including California and Florida, Japan and other breeding programs around the world (Fig. 1A, Table S1).  
115 Many cultivars were released between 1990s and nowadays, but the panel also accurately covered the  
116 whole modern breeding period (>1950s) and the early stages of strawberry breeding, with cultivars  
117 reaching as far as the beginning of the 19th century (Fig. S1). Thirty-two accessions from this panel were  
118 common with those from the study by Horvath et al. (2011)<sup>32</sup>. Accessions from the diversity panel were  
119 genotyped with the 50K FanaSNP array<sup>22</sup>. A total of 38,120 SNPs was retained after filtering for minor allelic  
120 frequency (MAF) (< 5%) and missing data (> 3%).

121 To explore relationships among the 223 accessions, we first evaluated the population structure with  
122 STRUCTURE software. We identified three distinct genetic clusters (Fig. 1B, Table S1). Group 1 (G1) includes  
123 most of the older European cultivars and their more recent relatives, as well as some old American cultivars  
124 (Fig. 1B). This group is hereafter named the Heirloom & related group. Group 2 (G2) clusters essentially  
125 European, as well as 14 American cultivars mostly from North-East America (Maryland, New-York and  
126 Canada) and three out of five Japanese cultivars (Fig. 1B) and was therefore named the European mixed

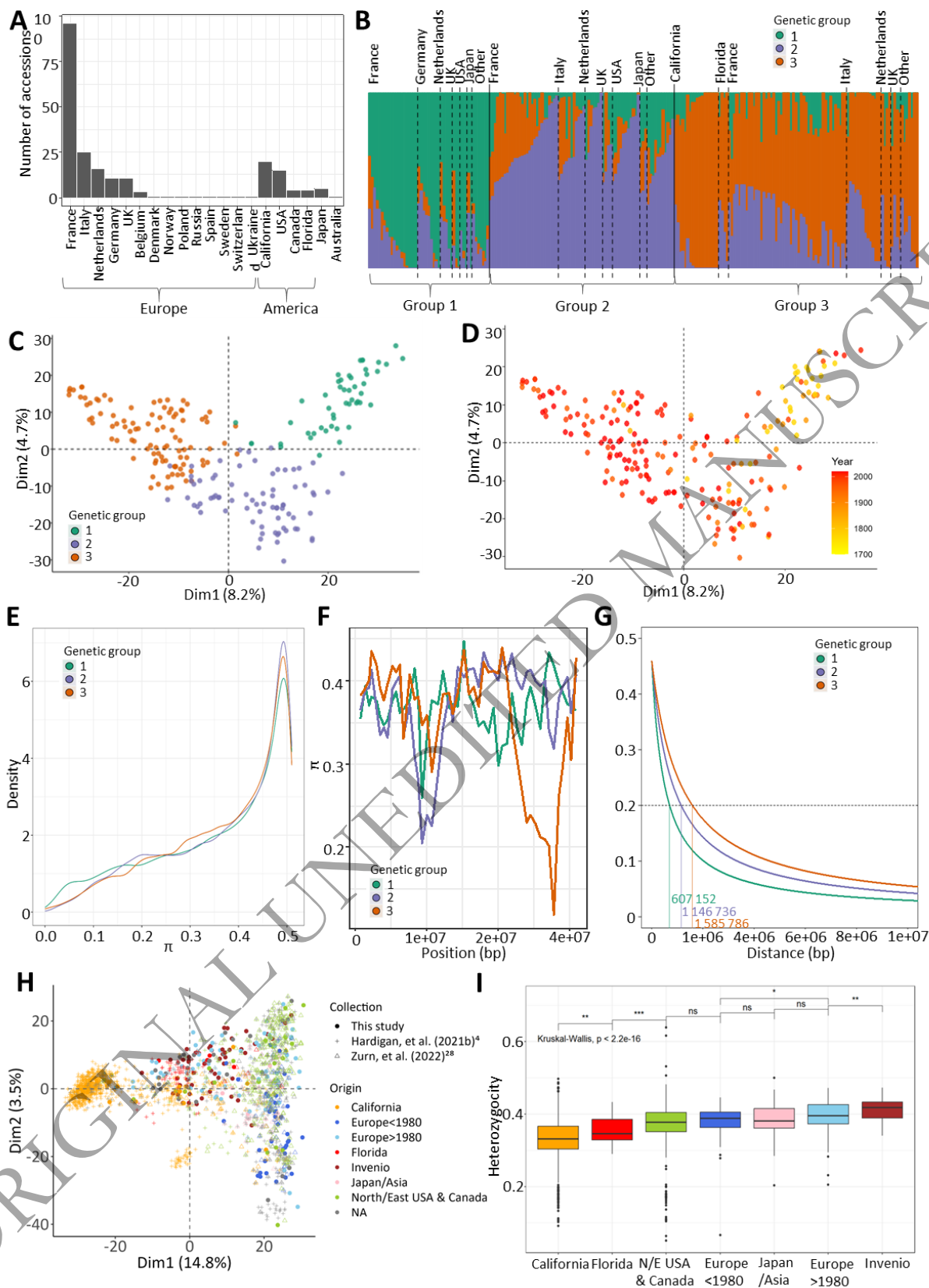
127 group. California and Florida cultivars, together with other European ones, have been identified in group 3  
128 (G3) hereafter named the American & European mixed group. A large amount of admixture (< 70%) was  
129 observed for each group, with 108 out of 223 accessions split across more than one group, with most of the  
130 admixture spread between G2 and G3 (Fig. 1B).

131 To further investigate population structure, we performed principal component analysis (PCA) of the 223  
132 accessions using the 38,120 SNP markers (Fig. 1C). The first two dimensions (PC1, PC2) explained 8.2% and  
133 4.7% of the structural variance, respectively. The three genetic groups were positioned at each vertex of  
134 the crescent shape. PC1 also reflected the temporal separation between G1 and the other two groups  
135 when cultivars were displayed according to year of release (Fig. 1D). The phylogenetic analysis (Fig. S2) was  
136 consistent with the structure (Fig. 1B) and PCA (Figs 1C, 1D) analyses.

137 Genome-wide comparisons of nucleotide diversity ( $\pi$ ) between genetic groups revealed no clear loss of  
138 genetic diversity from G1 to G2 and G3 (Fig. 1E). At the chromosome level, the distribution of nucleotide  
139 diversity among groups was uneven, with several genomic regions associated with significant enrichment  
140 or loss. Of notice, some regions were associated with a sharp reduction in diversity in G2 and/or G3  
141 compared with G1, for example the 23,233 kb to 29,635 kb region on chromosome 3D (Fig. 1F). Additional  
142 examples can be found on other chromosomes such as chromosomes 2C, 3B and 6B (Fig. S3). Progression  
143 towards the most recent American and European cultivars also translated in local augmentation in linkage  
144 disequilibrium, where LD (at  $r^2 = 0.20$ ) increased from an average distance of 802,184 bp for G1 to  
145 1,073,213 bp for G2 and 1,253,777 bp for G3 (Fig. 1G, Fig. S4).

146 We then combined the SNP data from our diversity panel with those from University of California Davis  
147 (UCD panel)<sup>4</sup> and United States Department of Agriculture (USDA panel)<sup>27</sup> to position our collection in  
148 relation with these studies. The PCA of the combined data revealed that the Invenio collection largely  
149 overlapped the two USA collections, with the exception of the extreme end of the PC1 corresponding to the  
150 UCD program and a small group of genotypes representing probable introgressions of wild accessions into  
151 the California panel (Fig. 1H, Fig. S5). The University of Florida (FL) program was less represented in the  
152 dataset, and closer to the UCD program on the PCA. Japanese and Asian varieties were located at the  
153 center of the crescent. In addition, the PCA highlighted the enrichment of our panel in unique  
154 accessions not found in the UCD and USDA panel, thus emphasizing its potential to find new phenotypic  
155 diversity for fruit quality traits in cultivated strawberry (Fig. 1H, Fig. S6). Heterozygosity decreased in  
156 California and Florida cultivars in comparison to European and Asian cultivars. Interestingly, heterozygosity  
157 was significantly higher in cultivars and advanced lines of Invenio and in recent European cultivars (released  
158 after 1980) (Fig. 1I).

159



160

161

162

163

**Figure 1.** Genetic diversity of the panel. (A) Distribution of the geographical origin of the 223 accessions. (B) Structure barplot representing each genotype (bars) by its percentage of affiliation to each of the three genetic groups according to the STRUCTURE analysis. Individuals are sorted by genetic groups and



164 geographical origins. (C,D) Principal Component Analysis of 38,120 SNP markers. Each accession (dot) is  
 165 colored by its genetic group (C) or year of release (D). (E) Nucleotide diversity ( $\pi$ ) distributions in windows  
 166 of 400 kb across each genetic group. (F)  $\pi$  chromosome-wide estimates for each genetic group for 400kb  
 167 windows across the chromosome 3D. (G) Linkage disequilibrium (LD) decay along chromosome 1A. The  
 168 dashed line represents the LD decay at  $r^2=0.2$ . (H) Distribution of the Invenio panel (filled dots) among  
 169 1,569 genotypes (shaded dots) studied in Hardigan et al. (2021b)<sup>4</sup> and 539 genotypes studied in Zurn et al.  
 170 (2022)<sup>28</sup> (shaded dots) with 3,215 SNP markers. Accessions are colored according to geographical/breeding  
 171 origin. (I) Heterozygosity coefficients across different geographical/breeding origins when combining  
 172 accessions from the diversity panel and 1,569 genotypes from Hardigan et al. (2021b)<sup>4</sup>.  
 173 Genetic groups 1, 2 and 3 are colored in green, purple and orange, respectively. Groups 1, 2, 3: Heirloom &  
 174 related, European mixed group and American & European mixed groups, respectively.

175

### 176 **Fruit quality traits in the diversity panel**

177 A total of 12 fruit quality traits were investigated in the panel of 223 accessions (Table 1). Traits were  
 178 related to fruit weight (FW); fruit appearance (COL, skin color; UCOL, uniformity of skin color; UFS,  
 179 uniformity of fruit shape; ACH, position and depth of achenes); firmness (FIRM); composition (TA, titratable  
 180 acidity; TSS, total soluble solids (Brix units), and BA, the deduced ratio (Brix/TA)); and skin properties (GLOS,  
 181 glossiness; SR, skin resistance; BRU, bruisedness). Analyses were carried out over two consecutive years,  
 182 with the exception of the FIRM and SR traits, which were assessed over a single year (Table 1).

183 Most of the traits exhibited a considerable range of variation in the diversity panel, with coefficients of  
 184 variation ranging from 3.7% for COL to 58.2% for skin resistance. For example, FW (average: 12.5 g) ranged  
 185 from 1.8 and 32 g. (Table 1). Most traits showed a normal distribution, while SR, GLOS, UFS and BRU  
 186 showed a skewed distribution (Fig. S6). Nine traits displayed high amount of genotypic variance associated  
 187 with high broad sense heritability ( $H^2$ ) ranging from 0.66 (ACH) to 0.98 (FIRM);  $H^2$  of four traits, namely UFS  
 188 (0.26), UCOL (0.43), BA (0.54) and BRU (0.57), was below 0.6 (Table 1). Few variations of  $H^2$  between groups  
 189 were observed for FW and FIRM, suggesting that phenotypic variability was equivalent between groups,  
 190 whereas a strongest decrease in  $H^2$  was observed for GLOS and BRU in G3 (Table 1). A significant interaction  
 191 between genotype and environment was detected for all the traits for which repeated measurements were  
 192 available over two years (Table 1), with the effect of environment being strongest for traits related to fruit  
 193 composition (TSS, TA, BA).

194 To further explore the phenotypes of the diversity panel, we performed a PCA of the 223 accessions using a  
 195 PCA biplot (Fig. 2A). PC scores revealed that the three genetic groups were distributed differently according  
 196 to PC1 (39.2%) and PC2 (17.2%) in terms of fruit quality traits. G1 was distinct from G2 and G3 (Fig. 1B, Fig.  
 197 S7A). Examination of the loadings of the traits on PC1 further showed that FW, appearance (UFS, UCOL),  
 198 FIRM and skin properties (GLOS, SR and BRU) traits were responsible for the separation between G1 on one



199 side and G2 and G3 on the other side. TSS, TA and ACH had a very small contribution to the differentiation  
 200 of the three subpopulations along PC1, and mostly contributed to PC2 and PC3, respectively (Fig. 2A, Fig.  
 201 S7B).

202

203 **Table 1.** Summary statistics of the 12 fruit quality traits evaluated on the diversity panel in 2020 and 2021.  
 204 n, number of accessions; CV, Coefficient of Variation; H<sup>2</sup>, broad sense heritability; H<sup>2</sup>G1, H<sup>2</sup>G2, H<sup>2</sup>G3, broad  
 205 sense heritability within each genetic group; %GE, percentage of genotype-by-environment interactions in  
 206 the total variance; r<sup>2</sup> structure, structuration of the trait as the coefficient of determination of the linear  
 207 regression between the trait values and the genetic groups. 20-21 indicates the combined values across  
 208 two years, 2020 and 2021. ns, not significant genotypic effect.

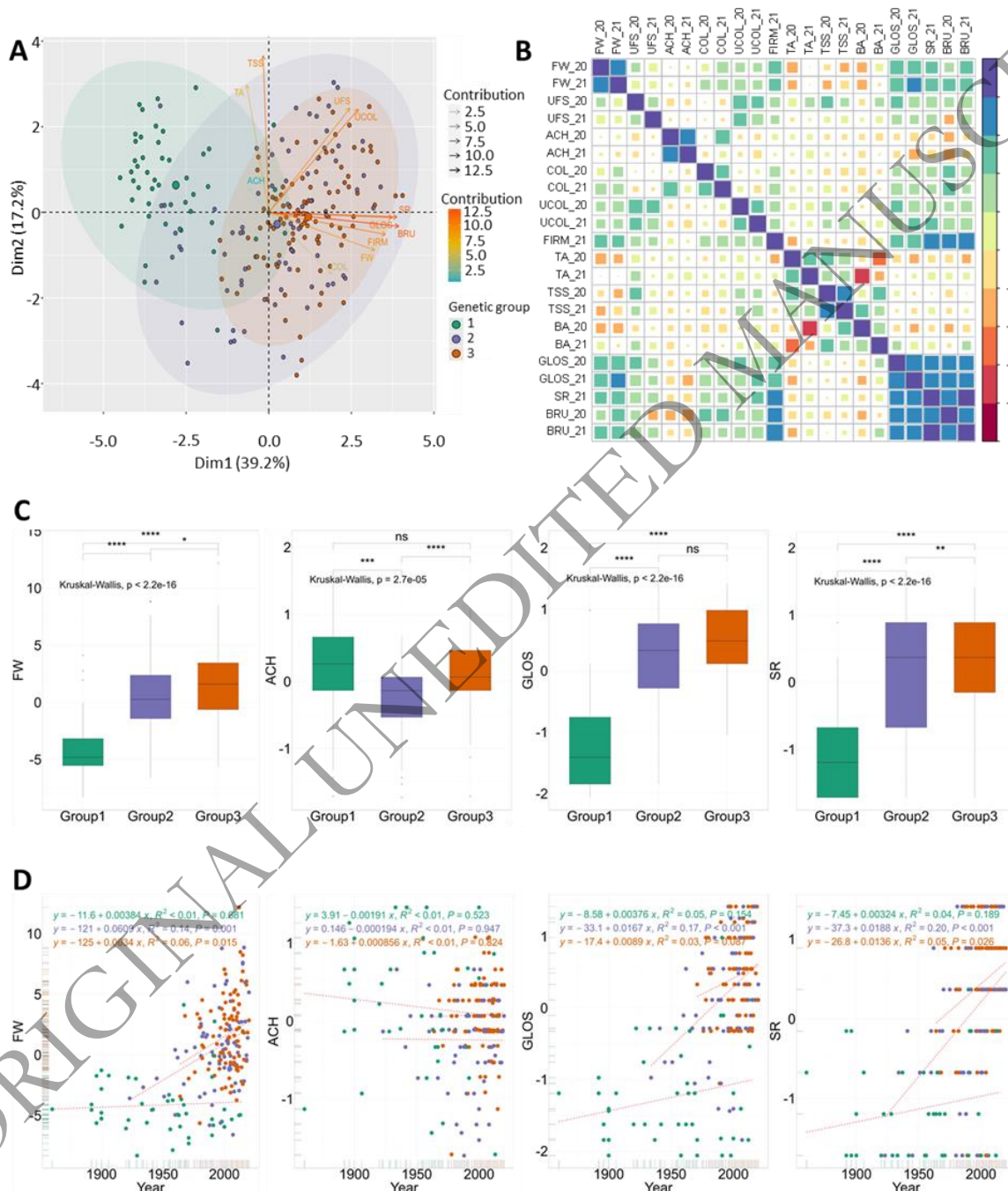
Trait	Year	n	Range	Mean	$\sigma$	CV	H <sup>2</sup>	H <sup>2</sup> G1	H <sup>2</sup> G2	H <sup>2</sup> G3	%GE	r <sup>2</sup> structure
Fruit weight (FW, in g)	2020	169	1.8 - 30.9	12.4	5.4	43.6	0.96	-	-	-	-	-
	2021	169	2.0 - 32.0	12.6	5.6	44.5	0.92	-	-	-	-	-
	20-21	169	1.8 - 32.0	12.5	5.5	44.1	0.81	0.71	0.68	0.71	23.4	0.30
Shape uniformity (UFS)	2020	208	1 - 5	2.7	1.3	48.0	-	-	-	-	-	-
	2021	197	1 - 5	3.1	1.3	41.5	-	-	-	-	-	-
	20-21	208	1 - 5	2.9	1.3	44.9	0.26	ns	0.50	ns	-	0.05
Achene position (ACH)	2020	209	1 - 5	3.5	0.8	23.3	-	-	-	-	-	-
	2021	198	1 - 5	3.2	0.9	28.8	-	-	-	-	-	-
	20-21	209	1 - 5	3.4	0.9	26.2	0.66	0.71	0.67	0.60	-	0.08
Skin color (COL)	2020	201	1 - 7	1.2	4.507	3.7	-	-	-	-	-	-
	2021	209	1 - 7.5	1.2	4.535	3.8	-	-	-	-	-	-
	20-21	209	1 - 7.5	1.2	4.522	3.8	0.68	0.77	0.67	0.60	-	0.03
Color uniformity (UCOL)	2020	208	1 - 5	3.0	1.3	42.7	-	-	-	-	-	-
	2021	198	1 - 5	2.8	1.3	47.0	-	-	-	-	-	-
	20-21	208	1 - 5	2.9	1.3	44.9	0.43	ns	0.59	0.32	-	0.10
Firmness (FIRM, in kg/mm)	2020	-	-	-	-	-	-	-	-	-	-	-
	2021	210	1.04 - 0.07	0.433	0.2	40.3	0.98	0.94	0.97	0.95	-	0.44
	20-21	-	-	-	-	-	-	-	-	-	-	-
Titratable acidity (TA, in g/L)	2020	195	0.7 - 2.3	1.4	0.3	20.6	0.83	-	-	-	-	-
	2021	175	0.4 - 2.0	1.2	0.3	24.1	0.91	-	-	-	-	-
	20-21	195	0.4 - 2.3	1.3	0.3	23.1	0.70	ns	0.85	0.82	34.5	0.03
Total soluble solids (TSS, in Brix)	2020	207	3.6 - 11.0	7.1	1.4	19.7	0.92	-	-	-	-	-
	2021	184	3.2 - 11.8	6.9	1.5	22.1	0.94	-	-	-	-	-
	20-21	207	3.2 - 11.8	7.0	1.5	20.9	0.78	0.68	0.83	0.75	30.2	0.04
Brix/acidity ratio (BA)	2020	195	2.9 - 7.9	5.1	1.0	19.9	0.87	-	-	-	-	-
	2021	175	2.1 - 12	5.6	1.5	27.5	0.95	-	-	-	-	-
	20-21	195	2.1 - 12	5.3	1.3	24.8	0.54	ns	0.85	0.51	48.5	0.00
Glossiness (GLOS)	2020	195	1 - 5	3.5	1.2	35.8	-	-	-	-	-	-
	2021	182	1 - 5	3.5	1.1	31.8	-	-	-	-	-	-
	20-21	195	1 - 5	3.5	1.2	33.8	0.77	0.76	0.64	0.43	-	0.48
Skin resistance (SR)	2020	-	-	-	-	-	-	-	-	-	-	-
	2021	210	0 - 3	1.65	1.0	58.2	-	-	-	-	-	0.34
	20-21	-	-	-	-	-	-	-	-	-	-	-
Bruisiness (BRU)	2020	199	1 - 5	2.5	1.3	50.8	-	-	-	-	-	-
	2021	54	0 - 5	1.8	1.0	54.3	-	-	-	-	-	-
	20-21	199	0 - 5	1.9	1.1	55.7	0.57	0.52	0.45	ns	-	0.49

209

210

211 Correlation analysis of fruit quality trait data collected over 2020 and 2021 (Fig. 2B, Table S2) supported the  
 212 relationships identified in the PCA biplot (Fig. 2A). GLOS, SR and BRU traits were positively and strongly  
 213 correlated with each other and with FW and FIRM ( $r=0.51$  to  $0.87$ ), indicating the strong potential for

214 directional selection of these traits (Fig. 2A). UFS and UCOL were also highly correlated among them  
 215 ( $r = 0.64$ ) and, to a lesser extent ( $r = 0.35$  and  $0.26$ ), with FW. TSS and TA were significantly correlated  
 216 ( $r = 0.45$ ) but, within groups, the correlation was only significant for G2 ( $r = 0.51$ ) and G3 ( $r = 0.47$ ) groups  
 217 (Fig. S8). FW also demonstrated significant negative correlations with TSS ( $r = -0.21$ ) and TA ( $r = -0.15$ ) (Fig.  
 218 2B; Table S2). No or weak correlations were observed between ACH and other fruit quality traits.  
 219



220  
 221 **Figure 2.** Phenotypic variations across the three genetic groups of the panel. (A) Principal Component  
 222 Analysis of the 2-year BLUP values for 11 traits. (B) Correlations between the 12 traits for each year. (C)  
 223 Comparisons of 2-year BLUP values for FW, ACH, GLOS and SR among genetic groups. (D) Genetic gains for

224 FW, ACH, GLOS and SR among genetic groups. Genetic groups 1, 2 and 3 are colored in green, purple and  
225 orange, respectively. Groups 1, 2, 3: Heirloom & related, European mixed group and American & European  
226 mixed groups, respectively. FW, fruit weight; UFS, uniformity of fruit shape; COL, skin color; UCOL,  
227 uniformity of skin color; ACH, position and depth of achenes; FIRM, firmness; TA, titratable acidity; TSS,  
228 total soluble solids; GLOS, glossiness; SR, skin resistance; BRU, bruisedness.

229  
230 Most fruit quality traits have undergone significant phenotypic changes over time, as old varieties have  
231 evolved into modern cultivars (Figs 2C, 2D, Fig. S9). Phenotypic values of all fruit quality traits, except BA  
232 and COL, were significantly different between the three genetic groups. For example, FW considerably  
233 increased during the modern breeding phase, as reflected mainly in trends within G2 and G3 (Figs 2C, 2D).  
234 G1 was associated with low FW, dull, soft, low SR and easily wounded skin with uneven color and shape,  
235 whereas G3 exhibited the highest values for these traits (Fig. 2C, Fig. S9). G2 was equivalent to G3 for UFS  
236 and UCOL, TSS and TA, and GLOS; and was in the average of G1 and G3 for FW, FIRM, SR and BRU. Cultivars  
237 from G2 displayed more outcropped achenes than the others (Fig. 2C, Fig. S9).

238 These changes are linked to significant genetic gains over time for most fruit quality traits, with the  
239 exception of ACH and BA (Fig. 2D, Fig. S10). For G2 and G3, the traits most affected along the breeding  
240 cycles were fruit appearance (GLOS, Fig. 2D; UFS and UCOL, Fig. S10), fruit resilience to transport and  
241 postharvest storage (SR, Fig. 2D; BRU and FIRM, Fig. S10) and fruit weight (FW, Fig. 2D). These traits are  
242 important for consumers, retailers and growers respectively. A negative, non-significant trend was however  
243 observed for TSS and TA, whose values were lower in G2 and G3 than in G1 (Fig. S9). Remarkably,  
244 regardless of the TSS and TA reduction in modern varieties compared to old varieties, no significant  
245 differences for BA values were observed between groups (Fig. S9).

246 While positive and time-dependent genetic gains were observed within G2 and G3, genetic gains were  
247 usually low or inexistent within G1. For FW, for example, several recent varieties of the G1 showed the  
248 same trait values as old ones. The absence of major improvements for such traits in modern cultivars  
249 belonging to G1 is probably due to a low selection pressure, as the main selection objective was to produce  
250 ornamental plants with pink flowers ('Frel' and 'Toscana') or white fruits ('Anablanca',  
251 'Blanche\_du\_Morvan', 'F\_Eure\_et\_Loire').

252

### 253 **GWAS of fruit quality traits**

254 To reveal the genetic architecture of fruit quality in strawberry, we performed GWAS on the 12 fruit quality  
255 traits assessed in the 223 accessions of the strawberry diversity panel using genome-wide SNP markers  
256 from the 50K FanaSNP array<sup>22</sup>. The structuration of the population (Figs 2B, 2C) was considered by fitting  
257 both kinship and structure as cofactors for GWAS analysis. Detailed Manhattan plots for all 12 traits are

258 shown in Figs 3, 4, Fig. S11. The 71 significant associations with SNP markers are distributed on 51  
259 chromosomal regions spread on 23 chromosomes (Table S3).

260

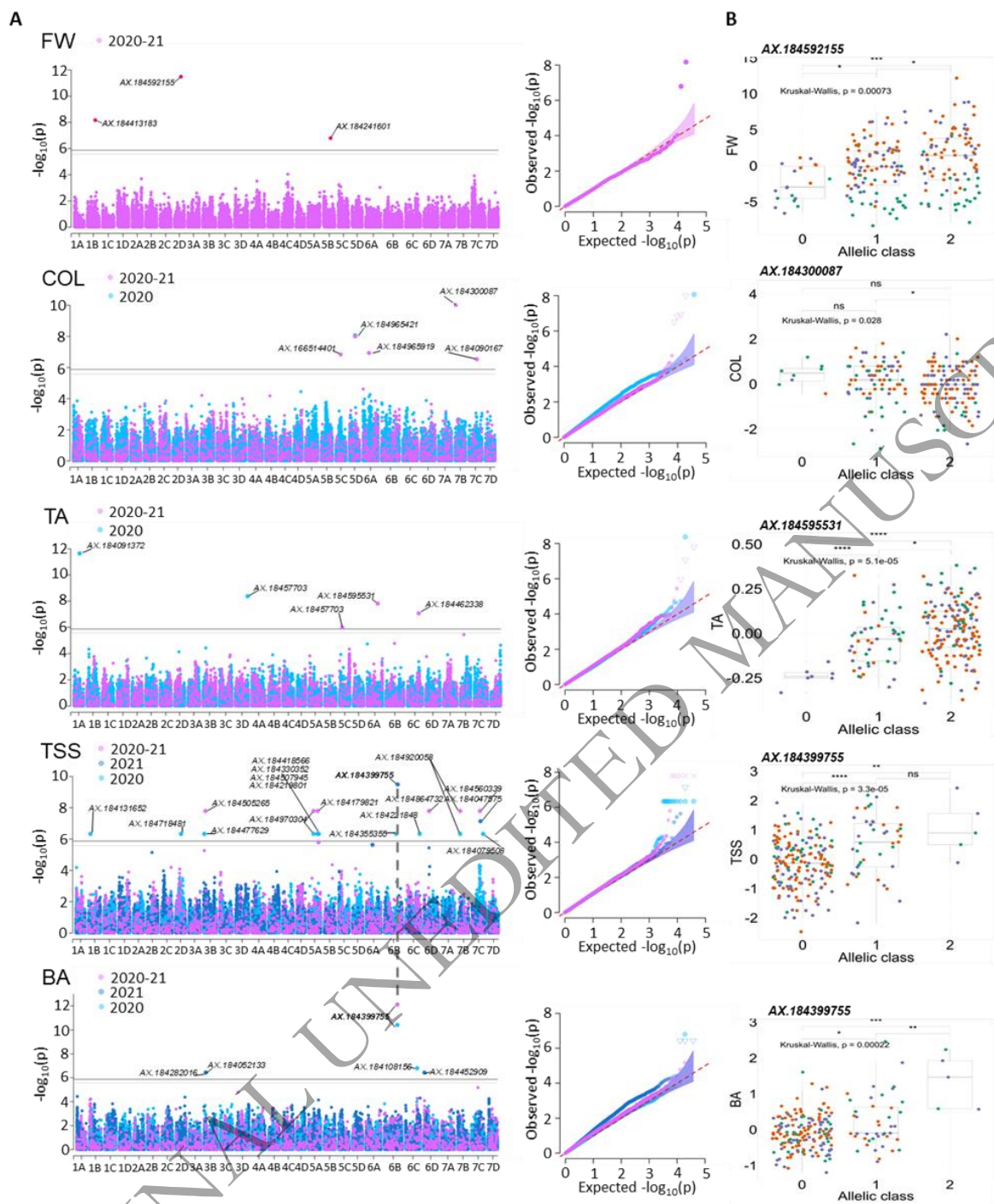
261 *Fruit weight and appearance (FW, UFS, COL, UCOL, ACH).*

262 Three significant SNP were identified for FW on chromosome 1B (19,119,571 bp, p-value 6.74E-09), 5B  
263 (17,045,086 bp, p-value 1.60E-06) and a highly significant SNP on chromosome 2D (15,565,564 bp, p-value  
264 3.27E-12) (Fig. 3A, Table S3). The minor allele of AX-184592155 had a phenotypic variance explained (PVE)  
265 of 11.8% with an effect of 1.8g on FW (Fig. 3B, Table S3). Sixteen unique significant SNPs were identified for  
266 appearance traits, eight for UFS, three for ACH and five for COL (Fig. 3A, Fig. S11, Table S3). No signal was  
267 detected for UCOL.

268

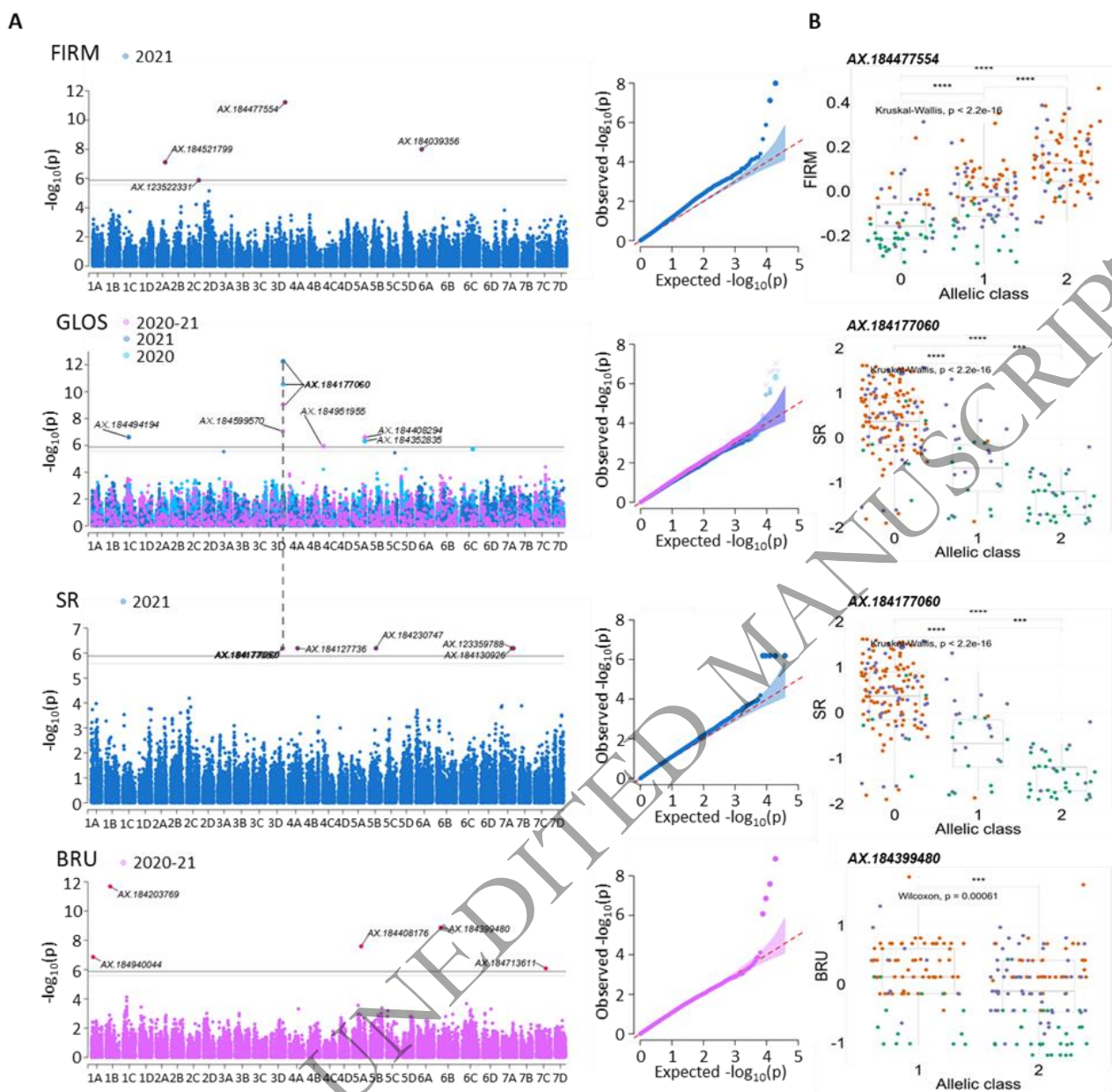
269

ORIGINAL UNEDITED MANUSCRIPT



270  
 271 **Figure 3.** Genome wide association study of FW, COL, TA, TSS and BA. (A) Manhattan and Q-Q plots for  
 272 yearly and 2-year BLUP values. (B) Effect of the most significant SNP marker. Genetic groups 1, 2 and 3 are  
 273 colored in green, purple and orange, respectively. Groups 1, 2, 3: Heirloom & related, European mixed  
 274 group and American & European mixed groups, respectively. FW, fruit weight; COL, skin color; TA, titratable  
 275 acidity; TSS, total soluble solids; BA, brix acidity ratio. Marker classes are as follows: 0=AA genotype, 1=AB,  
 276 and 2=BB genotype according to the Axiom™ Strawberry FanaSNP 50k.  
 277





278  
 279 **Figure 4.** Genome wide association study of FIRM, GLOS, SR and BRU. (A) Manhattan and Q-Q plots for  
 280 yearly and 2-year BLUP values. (B) Effect of the most significant SNP marker. Genetic groups 1, 2 and 3 are  
 281 colored in green, purple and orange, respectively. Groups 1, 2, 3: Heirloom & related, European mixed  
 282 group and American & European mixed groups, respectively. FIRM, firmness; GLOS, glossiness; SR,  
 283 skin resistance; BRU, bruisedness. Marker classes are as follows: 0=AA genotype, 1=AB, and 2=BB genotype  
 284 according to the Axiom™ Strawberry FanaSNP 50k.

285  
 286 *Fruit composition (TA, TSS, BA).*

287 Twenty-seven unique significant SNPs were detected for fruit composition traits, five for TA, 18 for TSS and  
 288 five for BA (Fig. 3A, Table S3). The SNP AX-184595531 detected for TA on the 2020-2021 combined values  
 289 (25,621,066 bp, p-value 1.55E-08) was particularly notable for its PVE of 35.5%. Only seven cultivars, all  
 290 belonging to G2, were unfavorable homozygous for this marker (Fig. 3B). SNPs AX-184091372 on

291 chromosome 1A (13,540,517 bp, p-value 2.30E-12, PVE 17.1%) and AX-184457703 on chromosome 3D  
292 (25,621,066 bp, p-value 4.22E-09, PVE 17.9%) were also of particular interest for their PVE and impacting  
293 effect on TA in 2021. AX-184399755 was the highest effect SNP for TSS in 2021 on chromosome 6B  
294 (31,578,303 bp, p-value 3.24E-10, PVE 19%) (Fig. 3B). It was also highly significant for BA in 2020 (p-value  
295 3.84E-11, PVE 46.1%) and 2020-2021 combined values (p-value 7.88E-13, PVE 65.8%) (Fig. 3B). Only five  
296 cultivars were favorable homozygous for this marker. Interestingly, the SNP markers associated with the  
297 TSS QTL on 6B (AX-184399755) and 6D (AX-184864732), and 7B (AX-184920058) and 7C (AX-184079508),  
298 were found very close on the diploid *F. vesca* reference genome (*F. vesca* v4.0.a1<sup>33</sup>), at 606,797 bp (Fvb6)  
299 and 449,220 bp (Fvb7) from each other respectively.

300

301 *Fruit firmness and skin properties (FIRM, GLOS, SR, BRU).*

302 Four significant SNPs were detected for FIRM, six for GLOS, five for SR and five for BRU (Fig. 4A, Table S3).  
303 The chromosome 3D was of particular interest for these traits as it comprises one highly significant SNP for  
304 FIRM (29,275,014 bp, p-value 6.07E-12, PVE 11.2%) and the highly significant SNP AX-184177060  
305 (27,845,440 bp) common to both GLOS (p-value 9.01E-10, PVE 26.2% on combined values) and SR (p-value  
306 6.45E-07, PVE 8.4%) (Fig. 4B). The latter SNP was detected systematically in 2020, 2021 and 2020-2021 for  
307 GLOS with PVE ranging from 26.2% to 28.7%, with a negative effect of the minor allele (-0.7 to -0.8 on 1 to 5  
308 scale). MAF of this SNP was highly reduced towards G3, indicating strong selection of the favorable allele  
309 (Fig. 4B). SNPs for BRU were detected for the 2020-2021 combined values only.

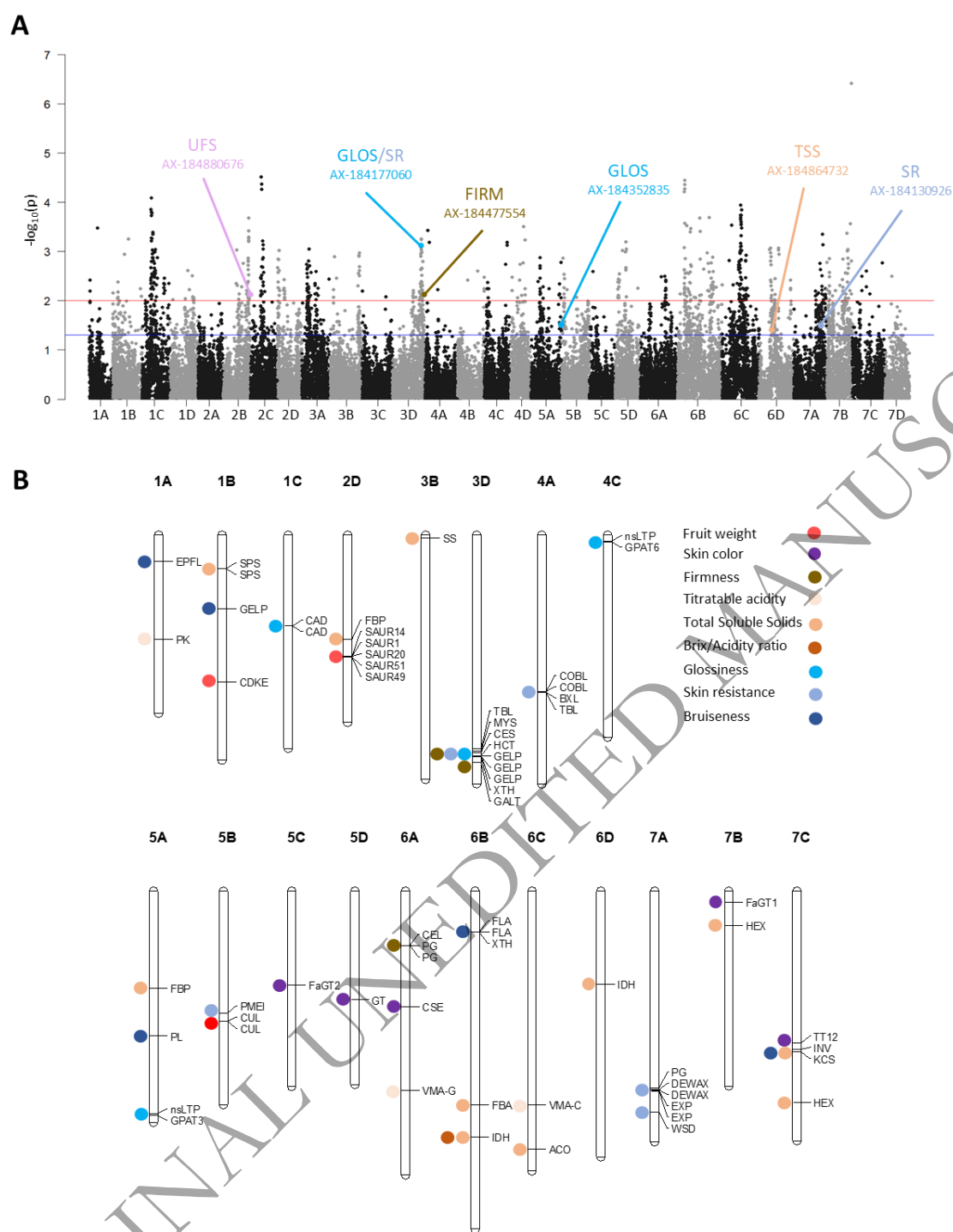
310

### 311 **Selective sweep signals during strawberry improvement**

312 We identified markers under selection during strawberry improvement in light of genome scans based on  
313 Mahalanobis distance across the diversity panel (Fig. 5A) and nucleotide diversity throughout the genome  
314 for all of the accessions in the diversity panel (Fig. 1F, Fig. S3). Six significant associations of SNP markers  
315 with fruit quality QTL were detected, including one for UFS, one for FIRM, one for TSS, two for GLOS and  
316 one for SR (Fig. 5A, Table S4). The AX-184177060 marker associated with GLOS and SR (chromosome 3D),  
317 the AX-184477554 associated with FIRM (chromosome 3D), and the AX-184864732 (chromosome 6D)  
318 associated with TSS, are found in chromosomal regions displaying a drastic reduction in nucleotide diversity  
319 in modern genotypes (Fig. 1F, Fig. S3, Table S4). For example, in the case of the SNP marker AX-184177060  
320 associated with the SR and GLOS QTL, the favorable allele is over-represented in the most recent accessions  
321 (average year of release 2000), whereas cultivars heterozygous or unfavorably homozygous for the marker  
322 were released around 1967 and 1947 respectively. This finding supports the fact that the favorable allele  
323 has been selected over time.

324





325

326

327

328

329

330

331

332

**Figure 5.** Selective sweeps and candidate genes. (A) Selective sweeps as a Manhattan plot of p-values of the genome scan based on Mahalanobis distance. Red and blue lines indicate thresholds at 0.01 and 0.05, respectively. Only significant (p-value < 0.05) SNP markers associated with fruit quality QTL are represented. UFS, uniformity of fruit shape; GLO, glossiness; SR, skin resistance; FIRM, firmness; TSS, Total soluble solids. (B) Physical mapping of the candidate genes underlying the GWAS of nine traits on the Camarosa genome. Full names and abbreviations of candidate genes are given in Table 2.

333  
334 **Candidate genes were identified for 37 QTL controlling 9 fruit quality traits**

335 Candidate genes (CG) underlying fruit quality QTL were identified within a window of ~400 kb surrounding  
336 the QTL marker. This value, which corresponds to the short-range LD found in the California cultivars of *F. ×*  
337 *ananassa*<sup>4</sup>, is stringent compared to the average LD calculated on the 28 linkage-groups in our diversity  
338 panel, which is 932 kb. In chromosomal regions harboring strong QTL of interest and displaying low genetic  
339 diversity and high LD, i.e. the 3D region extending from 23,233 to 29,635 kb (Fig. 1F), we considered much  
340 larger intervals based on LD estimates (up to ~1,382 kb) for 3B and 3D. We excluded two traits (UFS and  
341 ACH) from CG analysis because the molecular pathways underlying these traits are far from being  
342 deciphered in strawberry. No QTL was detected for UCOL. In total, we identified 64 candidate loci for 37  
343 SNP markers associated with the nine fruit quality traits (Fig. 5B). Table 2 provides names, abbreviations  
344 and positions on Camarosa and Royal Royce genomes of these 64 CG. Their possible functions are indicated  
345 in Table S5.

346  
347 **Table 2.** Candidate genes underlying nine fruit quality traits. PVE, Phenotypic variance explained (%).  
348 Position Camarosa and Position Royal Royce: physical positions on Camarosa and Royal Royce reference  
349 genomes. Protein encoded by the candidate gene (CG): annotation in the Camarosa genome. CG Position  
350 Camarosa and *F.x ananassa* identity: physical position and identity in the Camarosa genome. Published  
351 GWAS/QTL: QTL detected with Affymetrix strawberry arrays on the same chromosomal regions as in this  
352 study. \*, CG found outside ~400 kb intervals around SNP markers.

353

Trait	Chr	PVE	SNP marker	Position Camarosa	Position Royal Royce	Protein encoded by the Candidate Gene (CG)	CG Abbreviation	CG Position Camarosa	F.x ananassa identity	TAIR Arabidopsis homolog	Published Strawberry GWAS/QL a
Fruit weight (FW)	1B	5.5	AX-184413183	19 119 571	15 971 709	cyclin-dependent kinase E-1	<i>CDKE</i>	18 842 135	FxaC_2g34880	AT5G63610.1	
	2D	11.8	AX-184592155	15 565 564	8 801 569	small auxin upregulated RNA 14	<i>SAUR14</i>	15 581 781	FxaC_8g28530	AT4G38840.1	
						small auxin upregulated RNA 1	<i>SAUR1</i>	15 594 644	FxaC_8g28550	AT4G34770.1	
						small auxin upregulated RNA 20	<i>SAUR20</i>	15 611 587	FxaC_8g28590	AT5G18020.1	
						small auxin upregulated RNA 51	<i>SAUR51</i>	15 687 585	FxaC_8g28690	AT1G75580.1	
					small auxin upregulated RNA 49	<i>SAUR49</i>	15 697 093	FxaC_8g28700	FxaC_8g28700	AT4G34750.2	
	5B	3.6	AX-184241601	17 045 086	10 918 733	cullin	<i>CUL</i>	16 733 799	FxaC_18g25221	AT4G02570.4	
						cullin	<i>CUL</i>	16 708 079	FxaC_18g25150	AT4G02570.4	
Skin color (COL)	5C	1.7	AX-166514401	11 987 143	--	anthocyanidin 3-O-glucosyltransferase	<i>FoGT2</i>	12 158 604	FxaC_19g22400	AT5G17050.1	
	5D	3.8-23.4	AX-184965421	14022053	13542145	flavonoid 3-O-glycosyltransferase	<i>GT</i>	14049628	FxaC_20g25430	AT5G54010.1	
	6A	2.6	AX-184965919	14 476 176	21 070 121	caffeoylshikimate esterase	<i>CSE</i>	14 923 586	FxaC_21g30560	AT1G52760.1	
	7B	3.00986	AX-184300087	1386945	23020879	anthocyanidin 3-O-glucosyltransferase	<i>FoGT1</i>	1422660	FxaC_26g03070	AT5G17050.1	
	7C	9.9	AX-184090167	19 438 028	13 528 856	TT12-like MATE transporter	<i>TT12</i>	19 581 584	FxaC_27g28060	AT4G00350.1	
Firmness (FIRM)	3D	11.2	AX-184477554	29 275 014	2 454 715	AGP galactosyltransferase endotransglucosylase/hydrolase * cellulose synthase	<i>GALT</i> <i>XTH</i> <i>CES</i>	29 300 471 28 520 127 27 994 587	FxaC_12g45150 FxaC_12g43560 FxaC_12g42810	AT4G21060.2 AT3G23730.1 AT4G18780.1	
	6A	6.3	AX-184039356	7 277 130	27 533 782	cellulase 1 polygalacturonase polygalacturonase	<i>CEL</i> <i>PG</i> <i>PG</i>	7 038 578 7 048 245 7 054 511	FxaC_21g15730 FxaC_21g15750 FxaC_21g15770	AT1G70710.1 AT3G07820.1 AT3G07820.1	Cockerton et al. (2021); Hardigan et al. (2021b); Fan et al. (2024); Muñoz et al.
Titratable acidity (TA)	1A	17.1	AX-184091372	13 540 517	13 469 152	pyruvate kinase	<i>PK</i>	13 355 376	FxaC_1g27460	AT2G36580.1	
	6A	35.3	AX-184595531	25 621 066	9 172 070	V-type proton ATPase subunit G	<i>VMA-G</i>	25 704 934	FxaC_21g49700	AT3G01390.4	
	6C	6.8	AX-184462338	27 458 040	--	V-type proton ATPase subunit C	<i>VMA-C</i>	27 580 375	FxaC_23g44340	AT1G12840.1	
TSS (Brix)	1B	3.6	AX-184131652	4 174 690	1 302 571	sucrose-phosphate synthase sucrose-phosphate synthase	<i>SPS</i> <i>SPS</i>	4 316 703 4 319 488	FxaC_2g09440 FxaC_2g09441	AT5G20280.1 AT5G20280.1	
	2D	1.41107	AX-184718481	13298291	--	fructose-1,6-bisphosphatase, cytosolic	<i>FBP</i>	13361786	FxaC_8g25210	AT1G43670.1	
	3B	0.7	AX-184477629	1 541 393	1 842 542	* starch synthase	<i>SS</i>	453 429	FxaC_10g00830	AT4G18240.1	Fan et al. (2024)
	5A	0.9-2.1	AX-184970304	12400711	10544768	fructose-1,6-bisphosphatase, cytosolic	<i>FBP</i>	12546445	FxaC_17g26250	AT1G43670.1	
	6B	1.40326	AX-184355355	27647943	10765128	fructose-bisphosphate aldolase	<i>FBA</i>	27600407	FxaC_22g44640	AT3G52930.1	
	6B	18.9621	AX-184399755	31578303	9217798	isocitrate dehydrogenase [NAD]	<i>IDH</i>	31758475	FxaC_22g50900	AT5G03290.1	
	6C	0.58182	AX-184221848	33293635	29374007	aconitase	<i>ACO</i>	33266087	FxaC_23g56470	AT2G05710.1	
	6D	4.8	AX-184864732	12013420	9512125	isocitrate dehydrogenase [NAD]	<i>IDH</i>	11337718	FxaC_24g21140	AT5G03290.1	
	7B	1.6-4.0	AX-184920058	4515979	19984301	hexose carrier protein 6	<i>HEX</i>	4480262	FxaC_26g09610	AT5G61520.1	
	7C	7.71803	AX-184047575	20267768	--	alkaline/neutral invertase	<i>INV</i>	20384455	FxaC_27g29380	AT4G09510.1	
	7C	0.5	AX-184079508	26901718	13298291	hexose carrier protein 6	<i>HEX</i>	27292700	FxaC_26g09610	AT5G61520.1	
BA ratio	6B	65.8	AX-184399755	31 578 303	9 217 798	isocitrate dehydrogenase [NAD]	<i>IDH</i>	31 758 475	FxaC_22g50900	AT5G03290.1	
Glossiness (GLOS)	1C	17.8	AX-184494194	11 470 545	10 966 861	cinnamyl-alcohol dehydrogenase cinnamyl-alcohol dehydrogenase	<i>CAD</i> <i>CAD</i>	11 709 567 11 726 197	FxaC_3g21930 FxaC_3g21970	AT4G39330.1 AT4G37970.1	
	3D	4.7-28.7	AX-184599570- AX-184177060	26 901 693- 27 845 440	3 815 908-4 775 280	MYB-SHAQKYF trichome birefringence-like 38 * hydroxycinnamoyl-CoA shikimate/quinate * GDSL esterase/lipase * GDSL esterase/lipase * GDSL esterase/lipase	<i>MYS</i> <i>TBL</i> <i>HCT</i> <i>GELP</i> <i>GELP</i> <i>GELP</i>	27802931 27558105 28432367 28471370 28475004 28478770	FxaC_12g42500 FxaC_12g42010 FxaC_12g43430 FxaC_12g43470 FxaC_12g43480 FxaC_12g43490	AT2G38300.1 AT1G29050.1 AT5G48930.1 AT1G29670.1 AT1G29670.1 AT1G29670.1	
	4C	3.4	AX-184951955	727143	26073661	non specific lipid transport protein glycerol-3-phosphate acyltransferase	<i>nsLTP</i> <i>GPAT6</i>	756662 901347	FxaC_15g01440 FxaC_15g01830	AT2G37870.1 AT2G38110.1	
	5A	4.1-11.1	AX-184408294- AX-184352835	28658239- 28239789	24966878- 25341723	non specific lipid transport protein glycerol-3-phosphate acyltransferase	<i>nsLTP</i> <i>GPAT3</i>	28693018 28952583	FxaC_17g54360 FxaC_17g54920	AT5G64080.1 AT4G01950.1	
	3D	8.4	AX-184177060	27 845 440	3 815 908	MYB-SHAQKYF 1 trichome birefringence-like 38 shikimate/quinate hydroxycinnamoyltransferase * GDSL esterase/lipase * GDSL esterase/lipase * GDSL esterase/lipase	<i>MYS</i> <i>TBL</i> <i>HCT</i> <i>GELP</i> <i>GELP</i> <i>GELP</i>	27 802 931 27 558 105 28 432 367 28 471 370 28 475 004 28 478 770	FxaC_12g42500 FxaC_12g42010 FxaC_12g43430 FxaC_12g43470 FxaC_12g43480 FxaC_12g43490	AT2G38300.1 AT1G29050.1 AT5G48930.1 AT1G29670.1 AT1G29670.1 AT1G29670.1	
	4A	5.4	AX-184127736	20012930	16433479	COBRA-like COBRA-like beta-D-xylosidase trichome birefringence-like 43	<i>COBL</i> <i>COBL</i> <i>BXL</i> <i>TBL</i>	20088406 20089498 20219525 20238095	FxaC_13g38300 FxaC_13g38301 FxaC_13g38530 FxaC_13g38560	AT4G16120.1 AT4G16120.1 AT5G49360.1 AT2G30900.1	
	5B	3.6	AX-184230747	15853776	12173853	pectin methylesterase inhibitor	<i>PMEI</i>	15657184	D=FxaC_18g23430	AT5.1G38610	
	7A	7.3	AX-184130926	25616815	18667225	polygalacturonase expansin B2 expansin B2 decrease was biosynthesis 2 decrease was biosynthesis 2	<i>PG</i> <i>EXP</i> <i>EXP</i> <i>DEWAX</i> <i>DEWAX</i>	25398299 25744435 25766632 25608061 25647466	FxaC_25g46610 FxaC_25g47360 FxaC_25g47430 FxaC_25g47130 FxaC_25g47200	AT2G43890.1 AT1G65680.1 AT1G65680.1 AT5G07580.1 AT5G07580.1	
	7A	1.6	AX-123359788	28581204	--	wax ester synthase	<i>WSD</i>	28523042	FxaC_25g53661	AT3G49210.1	
	Bruisiness (BRU)	1A	6.91851	AX-184940044	3531536	--	epidermal patterning factor	<i>EPFL</i>	3396016	FxaC_1g08100	AT3G13898.1
1B		6.88666	AX-184203769	9439391	7276991	GDSL lipase	<i>GELP</i>	9476517	FxaC_2g20370	AT2G23540.1	
5A		4.38749	AX-184408176	18814640	16414924	pectate lyase	<i>PL</i>	18712472	FxaC_17g36850	AT5G09280.1	
6B		5.48905	AX-184399480	5731875	30532752	fascidin-like arabinogalactan protein fascidin-like arabinogalactan protein xyloglucan endotransglucosylase/hydrolase	<i>FLA</i> <i>FLA</i> <i>XTH</i> <i>XTH</i>	5305159 5332088 5351858 5351858	FxaC_22g11190 FxaC_22g11250 FxaC_22g11330 FxaC_22g11330	AT5G06920.1 AT5G06920.1 AT4G03210.1 AT4G03210.1	
7C		2.8	AX-184713611	20943204	15149370	3-ketoacyl-CoA synthase 1-like	<i>KCS</i>	20714519	FxaC_27g29940	AT1G01120.1	

<sup>a</sup>, Publications: Natarajan et al. (2020)<sup>41</sup>, Alarfaj et al. (2021)<sup>40</sup>, Cockerton et al. (2021)<sup>17</sup>, Hardigan et al. (2021b)<sup>4</sup>, Rey-Serra et al. (2021)<sup>15</sup>, Fan et al. (2023)<sup>29</sup>, Fan et al. (2024)<sup>31</sup>, Muñoz et al. (2024)<sup>3</sup>

355

356 **Discussion**

357

358 **Genetic and phenotypic shifts in modern strawberry breeding programs**

359 Our study sheds light on the genetic and phenotypic shifts that occurred over the last 160 years of  
360 strawberry breeding by analyzing 223 accessions comprising original old and modern European breeding  
361 material. According to our analyses, old strawberry cultivars, which here consist mainly of European  
362 cultivars selected before 1950 and included in the Heirloom & related group (G1), are clearly separated  
363 from other genetic resources (Fig. 1C), in agreement with earlier studies<sup>32</sup> confirmed in recent papers<sup>4,34</sup>.  
364 For over half a century<sup>35</sup>, breeding programs in Western and Southern Europe have made extensive use of  
365 California cultivars and, more recently, of Florida cultivars, which are underrepresented in our study, as  
366 progenitors. As a consequence, our results show the clustering of most European recent cultivars in an  
367 American & European mixed group (G3). The European mixed group (G2), which includes other European  
368 cultivars, is likely related to the group previously named Cosmopolitan<sup>4</sup>. European cultivars were also  
369 separated from US cultivars in the Zurn et al. (2022) study<sup>28</sup> due to the large number of American  
370 accessions.

371

372 The overall nucleotide diversity is well-conserved among the genetic groups of our panel (Fig. 1E). In  
373 contrast, a significant erosion of genetic diversity was observed in highly structured populations<sup>4,5,29</sup>. We  
374 found a more nuanced picture by examining nucleotide diversity at the chromosome level, since it drops  
375 dramatically in regions potentially subject to selection pressure (Fig. 1F, Fig. S3). The decrease in both LD  
376 and heterozygosity specifically observed in the most recent American cultivars<sup>4</sup> is likely explained by the  
377 gradual differentiation of California and Florida populations. In contrast, cultivars and advanced lines of  
378 Invenio as well as the recent European cultivars released after 1980 display higher heterozygosity values  
379 (Fig. 1I). One possible explanation for the high genetic diversity retained in European accessions is that  
380 European breeders had to cope with a wide range of breeding targets due to the diversity of cultural  
381 practices, markets and consumer preferences found in Europe<sup>6,36</sup>. High quality strawberry varieties released  
382 in Europe therefore had to meet the requirements of both high cultivar performance, e.g. high fruit yield,  
383 as in California cultivars<sup>5</sup> and high sensory fruit quality, e.g. high flavor<sup>6</sup>.

384

385 Remarkably, recent studies have shown that despite a loss in genetic diversity, increases in both genetic  
386 gain and phenotypic variation were observed in highly structured populations such as those of the  
387 California breeding programs<sup>5</sup>. In these programs, breeding efforts rapidly led to the improvement of fruit  
388 weight and fruit firmness<sup>5,27,29</sup>, which participated to the so-called California green revolution<sup>5</sup>. European  
389 breeding programs have benefited from these efforts, as modern American cultivars appear in the pedigree

390 of prominent European cultivars<sup>3</sup>. Consistently, our results indicate a similar trend towards improved fruit  
391 size and firmness, as well as skin glossiness and resistance, in recent European germplasm (Fig. 2C, Fig. S9).  
392 Interestingly, we found that TSS and TA values decreased over time in G1 but that the BA ratio kept the  
393 same value (Figs S9, S10), in agreement with Feldmann et al. (2024)<sup>5</sup> who even observed an increase in BA  
394 levels, which could partly counterbalance the decrease in fruit sweetness. Antagonism between yield and  
395 firmness, on one side, and TSS and TA, on the other side, was previously reported<sup>5,27,31</sup>.

396

### 397 **Novel markers for the selection of fruit quality traits**

398 GWAS is a powerful tool for the detection of SNP markers linked to different traits in strawberry<sup>9,17,29,31,37,38</sup>.  
399 Here, based on a large diversity panel, we detected 71 marker-associations to major fruit quality breeding  
400 targets. Some of the marker/QTL associations detected confirm published results and, consequently,  
401 validate our findings in a different genetic context. In comparison with the GWAS/QTL published  
402 data<sup>4,15,17,29,31,39,40,41</sup> obtained using the Affymetrix strawberry arrays, only two common fruit quality QTL  
403 located on the same chromosomal regions were detected here (Table 2). Our AX-184039356 marker linked  
404 to FIRM on 6A is very close to those previously described for fruit firmness<sup>4,17,31,39</sup>. Likewise, our AX-  
405 184477629 marker linked to TSS on 3B is in the same chromosomal region as the SSC1 QTL controlling  
406 soluble solids content<sup>31</sup>. In contrast, several previously reported QTL such as a FW QTL on 5B<sup>29,41</sup>, a TSS QTL  
407 on 5A<sup>41</sup>, a TA QTL on 5A<sup>15</sup> have been found on the same chromosomes but in different regions. The genetic  
408 diversity of unique European accessions included in our study allowed us to reveal new QTL and associated  
409 SNP markers, even for well-studied fruit quality traits such as FW and TSS.

410

411 In contrast to these well-studied traits, few studies have unveiled the genetic architecture of skin  
412 associated traits such as fruit glossiness<sup>17,42</sup> which is, alongside color, one of the most prominent traits for  
413 fruit attractiveness to the consumer<sup>43</sup>. Remarkably, of the six associations found among the selective  
414 sweeps detected, two were found for GLOS and one for SR (Fig. 5A). Furthermore, by highlighting a ~6,400  
415 kb region on chromosome 3D linked to glossiness, skin resistance and firmness, our results shed a new light  
416 on a genomic region under strong breeding pressure (Figs 1F, 5A). Remarkably, among the six associations  
417 found among candidate selective sweeps, two were found for GLOS and one for SR. This chromosomal  
418 region has thus probably played a crucial role in improving the attractiveness and post-harvest qualities of  
419 strawberries, a feature that is receiving increasing attention in strawberry breeding programs. Information  
420 on the position of SNP markers on both Camarosa and Royal Royce genomes will facilitate new studies on  
421 fruit quality traits, thus contributing to validate these markers for MAS.

422

### 423 **Candidate genes**

424

425 *Fruit weight and appearance*

426 Fruit weight (FW) and shape are complex traits. Underlying genes of previously unknown functions have  
427 been identified by map-based cloning in species such as tomato<sup>44</sup> and corresponding CG have been  
428 detected in several crops<sup>45</sup>. Translation of these findings to strawberry may however prove difficult because  
429 of the different ontogenic origin of strawberry, which is an accessory fruit derived from the flower  
430 receptacle and not from the ovary. Indeed, our GWAS study did not detect any known gene families linked  
431 to fruit weight and shape, but highlighted for FW QTL several CG (*CDKE*, a cluster of five *SAUR*, *CUL*)  
432 involved in cell division and expansion processes and their regulation (Table S5).

433

434 Red-colored anthocyanins, which give strawberries their attractive bright red appearance, are flavonoids  
435 derived from the phenylpropanoid pathway. In cultivated strawberry, allelic variants of the master  
436 regulator *MYB10* belonging to the MBW complex have been shown to be responsible for the white skin-  
437 color and red flesh-color<sup>8,11</sup>. In our GWAS study, we did not detect any previously known color QTL nor CG  
438 linked to the MBW complex, probably because white fruit genotypes and flesh-color trait were under-  
439 represented in our analysis. However, our diversity panel has enabled us to reveal new skin color QTLs and  
440 identify strong CG involved in the successive steps leading to anthocyanin accumulation in strawberry<sup>11</sup>: (i)  
441 anthocyanin biosynthesis; (ii) formation of stabilized anthocyanidin-glucosides; and (iii) transport of  
442 anthocyanidin-glucosides for storage in the vacuole. Color CG, which deserve further study, include a gene  
443 (*CSE*) encoding shikimate esterase, an enzyme involved in lignin pathway that may compete with  
444 anthocyanin biosynthesis for common substrates; several genes encoding glycosyltransferases (*GT*), among  
445 which the strawberry FaGT1 enzyme that has been shown to generate anthocyanidin 3-O-glucosides<sup>46</sup> and  
446 its homolog FaGT2; and a gene encoding a vacuolar flavonoid/H<sup>+</sup>-antiporter (*TT12*) that can actively  
447 transport cyanidin-3-O-glucoside to the vacuole<sup>47</sup>.

448

449 *Fruit firmness and composition*

450 Breakdown of the cell wall (CW) is the main mechanism responsible for fruit softening during ripening. CW  
451 is mainly constituted by a cellulose-hemicellulose network immersed in a pectin matrix. Strawberry fruit  
452 softening involves the pectin-degrading enzymes polygalacturonase (PG) and pectate lyase (PL)<sup>48</sup>. The  
453 down-regulation of *PL*<sup>49</sup> and of *PG*<sup>50</sup> influences fruit firmness and/or shelf life of strawberry. Many  
454 additional proteins are involved in CW modifications e.g. pectin methylesterase (PME) and its inhibitors  
455 (PMEI) that control cell adhesion and elasticity through pectin esterification, enzymes of the xyloglucan  
456 endotransglycosylase/hydrolase (XTH) family involved in hemicellulose remodelling, cellulases (CEL) that  
457 degrade cellulose, and expansins (EXP) that promote CW loosening. Other enzymes such as cellulose  
458 synthase (CES) or proteins with ill-defined roles such as arabinogalactan-proteins (AGPs) likely play a role in  
459 CW structure and properties. Therefore, considerable variations in fruit firmness can be expected by

460 modulating the activity of enzymes encoded by CG underlying the 3D QTL (*GALT*, *XTH*, *CES*) and 6A (*CEL*,  
461 *PG*) QTL. *XTH* and *CES* are strong candidates located at 750 to 1,280 kb from the AX-184477554 marker in  
462 the well-conserved 3D region while *CEL* and *PG* underly the 6D FIRM QTL previously detected<sup>4</sup>.

463

464 The sugar/acid balance is central for consumers perception of fruit quality<sup>19</sup> and the sugar/acid ratio has  
465 been widely adopted as a breeding target<sup>5</sup>. The major soluble sugars that accumulate during fruit ripening  
466 are glucose, fructose and sucrose, the concentration of which depends on the cultivar<sup>51</sup>. The major organic  
467 acids are malate and especially citrate, which is the predominant organic acid<sup>48</sup>. Their concentrations are  
468 stable or decrease during fruit ripening. Fruit sweetness is usually assessed in refractometer (Brix units),  
469 which measures total soluble solids (TSS), including sugars and organic acids. Fruit acidity is assessed by TA,  
470 to which citrate contributes most in strawberry. The accumulation in strawberry of soluble sugars and  
471 organic acids depends on synthesis in the leaf (source) and long-distance transport of photoassimilates  
472 (sucrose, inositol) to the fruit (sink). Photosynthetic sugars are further metabolized in the fruit to produce  
473 soluble sugars and organic acids that are then stored in the vacuoles<sup>52</sup>. Our GWAS study identified several  
474 CG implicated in the metabolism of sugars, either in the leaves or in the fruit, including *SPS* (1B QTL), *FBP*  
475 (2D and 5A QTL), *SS* (3B QTL), *FBA* (6B QTL), and *INV* (7C QTL). The starch synthase (*SS*) is located more than  
476 1 Mb apart from the 3B QTL marker but has been recently identified as a CG for a TSS QTL<sup>31</sup>. The neutral  
477 invertase (*INV*), which underlies the major 7C TSS QTL (PVE 7.7%), is a strong candidate that has been  
478 shown to be crucial for glucose and fructose accumulation during ripening in tomato<sup>53</sup> while a cell wall  
479 invertase is responsible for a major TSS QTL in this species<sup>54</sup>. Another strong candidate is the hexose  
480 transporter (*HEX*) (7B and 7C QTL), which could transport glucose and fructose across the tonoplast, as  
481 suggested in grape berries<sup>55</sup>. Furthermore, the *HEX* gene may underlie two possible TSS homoeo-QTL  
482 located on chromosomes 7B and 7C, respectively.

483

484 Two CG underlying TSS QTL encode enzymes involved in the tricarboxylic acid (TCA) cycle, notably isocitrate  
485 dehydrogenase [NAD] (*IDH*) (6B QTL) and aconitase (*ACO*) (6C QTL). TCA is the central metabolic cycle that  
486 uses substrates from the glycolysis to produce energy. It fulfills major roles in the fruit, among which the  
487 metabolism of citric acid<sup>56</sup>. While aconitase has been shown to contribute to the regulation of acidity in the  
488 citrate-accumulating lemon<sup>57</sup>, we did not detect any TA QTL corresponding to the 6C Brix QTL. Interestingly,  
489 *IDH* underlies strong shared QTL for TSS (PVE=19.0) and BA (PVE=65.8) on chromosome 6B. The implication  
490 of *IDH* a significant contributor to the TCA cycle, in the sugar/acid balance of strawberry, therefore merits  
491 further studies. Moreover, *IDH* is also located at ~ 675 kb from the TSS QTL on chromosome 6D, indicating  
492 that it could underlie two TSS homoeo-QTL located on chromosome 6B and 6D, respectively. As previously  
493 suggested<sup>13</sup>, the detection of homoeo-QTL could depend on environmental conditions, which vary  
494 according to the year of study.



495

496 The CG underlying the 1A TA QTL encodes pyruvate kinase (PK) a crucial enzyme for gluconeogenesis which  
497 has already been demonstrated to regulate citric acid metabolism during strawberry fruit ripening<sup>56</sup>. Two  
498 additional CG for the TA QTL located on 6A (PVE 35.3%) and 6C (PVE 6.8%) encode subunits of the V-type  
499 proton ATPase (*VMA-G* and *VMA-C*), respectively. Both are strong candidates for the control of fruit acidity,  
500 as they are part of a protein complex whose role is to generate a proton gradient across the tonoplast,  
501 which is essential to drive the storage of organic acids in the vacuole of fleshy fruits<sup>58</sup>.

502

### 503 *Skin properties*

504 The outermost wall of the fruit is composed of the cuticle, the epidermis and several layers of sub-  
505 epidermal cells<sup>59</sup>. This ill-defined tissue, also called fruit skin<sup>60</sup>, acts as a barrier against water-loss and  
506 pathogens and provides protection against mechanical injuries<sup>61</sup>. Its properties depend on epidermal and  
507 sub-epidermal cell patterning (cell size and shape) and on the composition and structure of CW and cuticle.  
508 To date, the cuticle has been poorly studied in strawberry, except for its composition<sup>62</sup>. Recent studies, in  
509 particular in the tomato model, furthered our understanding of the synthesis of cuticle components (wax  
510 and cutin polyester, phenolics) and explored the complex interactions between cutin polyesters, CW  
511 polysaccharides and phenolics, and their possible contribution to cuticle properties<sup>59</sup>.

512

513 Fruit glossiness is an environment-sensitive trait linked to wax and cutin accumulation on the fruit surface  
514 but also to epidermal cell patterning<sup>63</sup>. Among CG identified for GLOS QTL are genes involved in  
515 phenylpropanoid pathways (*CAD* in 1C QTL), epidermal patterning (*TBL* in 3D QTL), regulation of wax  
516 biosynthesis (*MYS*, 3D QTL), lipid and cutin biosynthesis (*GPAT6*, 4C QTL; *GPAT3*, 5A QTL) and possibly  
517 transport of cutin precursors (*InsLTP*, 4C and 5A)<sup>61,64</sup>. In addition to the *MYS* gene, a transcription factor  
518 involved through *DEWAX* in the regulation of the *ECERIFERUM1* (*CER1*) enzyme involved in the biosynthesis  
519 of wax alkanes<sup>65</sup>, this region harbors, within ~700 kb of 3D QTL markers, the phenolic pathway *HCT* gene  
520 that is essential for cuticle formation<sup>66</sup> and, close-by, three *GELP* genes. Several members of the large *GELP*  
521 family have been demonstrated to play crucial roles in cutin polymerization (cutin synthase<sup>67</sup>) and in  
522 assembly-disassembly of the related polyester suberin<sup>68</sup>. Examination at the Tomato eFP Browser  
523 (<http://bar.utoronto.ca>) and TEA-SGN (<https://tea.solgenomics.net>) databases of the expression of the  
524 three closest tomato homologs (*Solyc03g005900*, *Solyc02g071610*, *Solyc02g071620*) of the 3D GLOS QTL-  
525 linked *GELP* genes indicate that they are strongly expressed in the young fruit, when the cutin synthesis  
526 rate is the highest<sup>63</sup>. Furthermore, in the tomato pericarp, their expression is restricted to the outer and  
527 inner epidermis. These findings strongly suggest that, in cultivated strawberry, a cluster of genes with likely  
528 roles in cuticle formation and structure has been selected in modern varieties for its impact on fruit cuticle-  
529 related traits, including GLOS.

530

531 Remarkably, we found that the major skin resistance (SR) QTL, which estimates the fragility of the fruit  
532 surface to peel off when a mechanical stress is applied, is shared with the GLOS QTL on 3D. The major 3D  
533 FIRM QTL (PVE 11.2%) was also found nearby (at ~1,400 kb). Since the FIRM trait was estimated by  
534 measuring the force needed to punch a hole in the fruit surface (penetrometer), it can be linked to the  
535 properties of the fruit skin. Interestingly, connections between fruit firmness and the cuticle have recently  
536 been demonstrated in tomato where changes in cuticle composition and properties are responsible for a  
537 major firmness QTL<sup>69</sup>. Altogether, these results suggest that in the 3D conserved region, modifications of  
538 fruit surface properties, either due to changes in epidermal cell patterning and/or in cell wall and cuticle  
539 properties, have been selected in modern strawberry varieties for their effect on both fruit glossiness,  
540 resistance to mechanical damages, and possibly firmness. Other candidates linked to either epidermis  
541 patterning (*TBL* on 4A), cell wall modifications (*COBL* and *BXL* on 4A, *PMEI* on 5C, *PG* and *EXP* on 7A) and  
542 cuticle formation (*DEWAX*, a target of *MYS*, and *WSD* on 7A) underly the additional SR QTL detected.

543

544 In contrast, none of the QTL detected for fruit bruisedness (BRU), a trait assessed visually, were found to  
545 co-localize with either GLOS, SR or FIRM QTL while all these traits are strongly correlated, indicating that  
546 the underlying mechanisms are probably different or that the corresponding QTL are below the detection  
547 threshold. CW-related GC that may affect cell wall properties (*PL* on 5A, *XTH* on 6B) or cell adhesion of sub-  
548 epidermal cells (*FLA* on 6B<sup>70</sup>) merit further investigation, as fruit susceptibility to bruising is essential for  
549 post-harvest handling and defense against fruit decay.

550

## 551 Conclusion

552 In summary, the exploration of untapped genetic resources, including European cultivars spanning 160  
553 years of breeding, has revealed considerable changes in recent decades in the genetic and phenotypic  
554 diversity of cultivated strawberry. American cultivars have had a major impact on recent European  
555 breeding programs and, therefore, on modern strawberry varieties in Europe. However, our findings also  
556 revealed that a considerable, and previously undescribed, genetic diversity can be harnessed for improving  
557 fruit quality through breeding. Our study also highlights the contribution of fruit surface traits (glossiness,  
558 skin resistance, bruisedness) to the development of modern varieties. The strong CGs underlying the main  
559 QTL detected for these little studied traits warrant further investigations. This can be done, for example,  
560 through additional association studies or functional analyses. From a more applied perspective, the genetic  
561 markers highlighted will be used for the selection of improved strawberry varieties with high fruit quality.

562

## 563 Materials and methods

564

565 **Plant materials and experimental design**

566 A total of 223 accessions from the historical germplasm collection of Invenio was chosen to constitute the  
 567 diversity panel. The trial took place in a soilless system, at Douville in the South-West of France (45° 1.2831'  
 568 N; 0° 37.0198' E, France). The crop management was the one used for commercial semi-early cultivated  
 569 strawberry in France. The trial was organized in a randomized complete block design of two blocks of four  
 570 biological replicates each in a 288 m<sup>2</sup> glass greenhouse in 2020 and 2021. Planting of tray plants occurred  
 571 around the 15<sup>th</sup> of December of the previous year.

572

573 **Sample preparation and phenotyping**

574 Fruits were harvested once per season and evaluated for 12 fruit quality traits: FW, fruit weight; UFS,  
 575 uniformity of fruit shape; COL, skin color; UCOL, uniformity of skin color; ACH, position of achenes; FIRM,  
 576 firmness; TA, titratable acidity; TSS, total soluble solids; BA, TSS/TA ratio; GLOS, glossiness; SR, skin  
 577 resistance; BRU, bruisedness. FW was evaluated as the mean weight of harvested fruits after discarding  
 578 immature and overripe fruits. UFS, UCOL, ACH as well as GLOS and BRU were visually assessed on 1-5 scales  
 579 (Table 1) as a single note on a whole strawberry tray (>10 red ripe fruits). COL was evaluated on 4-5 red ripe  
 580 fruits a 1-8 scale based on the strawberry color chart from Ctifl  
 581 (<http://www.ctifl.fr/Pages/Kiosque/DetailsOuvrage.aspx?IdType=3&idouvrage=833>). FIRM was evaluated  
 582 on six fruits from each accession with an FTA-GS15 (Güss) penetrometer (5 mm diameter) at 3 mm depth (5  
 583 mm/s speed, 0.06kg release threshold). SR was evaluated on three fruits per accession on a 1-5 scale by  
 584 applying an ascending pressure with the extremity of the thumb on the fruit surface. Bruisedness, which  
 585 represents the susceptibility of the fruit to mechanical damages, was evaluated by visual inspection of the  
 586 fruits 4 h after harvest. Analyses were performed for two consecutive years except for FIRM and SR traits  
 587 which were evaluated a single year in 2021. TA and TSS were evaluated from a homogenized pool of a  
 588 minimum of 10 fruits with a pH-metric titration with sodium hydroxide of 10 g fruit puree and an Atago  
 589 Handheld (PAL-1) Digital Pocket Refractometer (Atago, Saitama, Japan), respectively.

590

591 **Statistical analysis**

592 Best Unbiased Linear Predictors (BLUPs) for the diversity panel were calculated using a linear mixed model  
 593 (LMM) from the lme4 R package<sup>71</sup>:

594

$$y_{ijkl} = \mu + G_j + B_k + Y_l + (G : Y)_{il} + \epsilon_{ikl}$$

595 where Y/E represented the fixed effects of year/environments; B the fixed effect of blocks; G the  
 596 random genotypic effect, with  $G \sim N(0, \sigma_G^2)$ ; GxY/E the random genotype x year/environment effects, with  
 597  $GxY/E \sim N(0, \sigma_{Y/E}^2)$ ;  $\epsilon$  the residual term, with  $\epsilon \sim N(0, \sigma_e^2)$ .

598

599 Variance components for these effects were estimated using restricted maximum likelihood (REML).

600 Broad sense heritability was estimated as follows:

$$H^2 = \frac{\sigma^2 G}{\sigma^2 G + \frac{\sigma^2 G:Y}{nyear} + \frac{\sigma^2 e}{nyear \times nrep.year}}$$

601 where genotype (G) variance at the numerator. Random variance components involving year (Y) were  
602 divided by the mean number of years (*nyear*). Other random variance components involving block effects  
603 or residuals were divided by the mean number of years times the mean number of replicates per year  
604 (*nrep.year*).

605 Pearson correlation between different traits were calculated using 'cor' function and visualized by 'corrplot'  
606 v. 0.92 R package. PCA on all traits was performed using the prcomp function from R core and visualized  
607 with fviz\_pca function from factoextra v.1.0.7 package or ggplot2 package. The impact of the structure on  
608 each variable was assessed by simple regression of the genetic groups on their respective phenotypes.

609

### 610 Genotyping

611 DNA was extracted from young leaves with a CTAB method adapted from Sánchez- Sevilla *et al.*, (2015)<sup>34</sup>.  
612 Samples were genotyped using Affymetrix® 50K FanaSNP array<sup>22</sup> in the 'Gentyane' genotyping platform  
613 (Clermont-Auvergne-Rhône-Alpes, INRAE, France). SNP calling was processed through Axiom™ Analysis  
614 Suite software (v5.1.1.1; Thermo Fisher Scientific, Inc.) following the best practices of the software  
615 documentation. Accessions with missing data higher than 3% were removed from analysis. Markers  
616 presenting more than 5% of missing data and minor allele frequencies of less than 5% were filtered out.

617

### 618 Structure and genetic diversity analysis

619 We performed a structure population analysis using STRUCTURE (v2.3.4<sup>72</sup>) with 5 runs for a range of K = 2  
620 to 10 with 38,120 markers. The burn-in period length was set to 10,000 and 20,000 Markov Chain Monte  
621 Carlo (MCMC). The best fitting K was identified with STRUCTURE HARVESTER<sup>73</sup>. Plots were performed using  
622 the ggplot2 v.3.3.6 package<sup>74</sup>. PCA analyses were performed with PCA function from factorMinerR v.2.7  
623 package<sup>75</sup>. Additionally, we included genotypes from Hardigan *et al.*, (2021b)<sup>4</sup> and Zurn *et al.* (2022)<sup>28</sup> to  
624 perform PCA using the prcomp function from R core and visualize with fviz\_pca\_ind function from  
625 factoextra v.1.0.7 package or ggplot2 package. We conducted a ML tree with the 233 accessions using IQ-  
626 TREE v.2.1.3<sup>76</sup> with 1000 bootstrap and the TVMe+ASC+R3 model suitable for SNP arrays. Linkage  
627 disequilibrium for each chromosome and genetic group was computed using the LDcorSV v.1.3.3 package<sup>77</sup>.  
628 Nucleotide diversity among each genetic group was calculated using TASSEL<sup>78</sup>. Finally, we performed  
629 principal component analysis-based genomes scans to detect markers under selection using the pcadapt  
630 package<sup>79</sup>, implementing the pcadapt function with K = 3. Output from genome scans were then compared  
631 with nucleotide diversity profiles to search for selective sweeps.

632

### 633 **Genome-Wide Association Study**

634 The association mapping was performed using GAPIT v.3<sup>80</sup> using the Camarosa genome physical positions<sup>1</sup>  
635 with the Bayesian-information and linkage-disequilibrium iteratively nested keyway (BLINK) model<sup>81</sup>. In  
636 order to control for confounding effects, the structure was implemented for each trait in two different  
637 ways by 1) adding the previously calculated structure parameters as covariates or 2) fitting directly principal  
638 components from the principal component analysis using the PCA.total argument. Best models were  
639 selected based on genomic inflation factors,  $\lambda$ . The kinship was determined from the SNP data using the  
640 VanRaden mean algorithm. The analysis was performed on yearly and across two years Best Linear  
641 Unbiased Predictors (BLUPs), using a 5% Bonferroni threshold. Manhattan and Quantile-Quantile plots  
642 were plotted using the CMplot R package. Allelic effects for each significant marker were plotted on  
643 adjusted means using the ggplot2 R package.

644

### 645 **Candidate gene mining**

646 Candidate genes (CG) underlying fruit quality QTL were identified in intervals of ~400 kb around the QTL  
647 marker. This value, which corresponds to the short-range LD found in California cultivars of *F. × ananassa*<sup>4</sup>,  
648 is stringent compared to the average LD of 932 kb calculated in our diversity panel. In chromosomal regions  
649 harboring strong QTL of interest and displaying low genetic diversity and high LD, larger intervals (up to  
650 1,382 kb) were considered. The annotations of genes located within the QTL interval were retrieved from  
651 *F. × ananassa* cv. Camarosa reference genome assembly v1.0<sup>1</sup> and cv. Royal Royce haplotype-resolved  
652 genome v1.0 assembly<sup>23</sup>. Based on the authors' expertise in fruit biology, QTL intervals were first inspected  
653 manually for genes belonging to categories possibly related to fruit quality traits, e.g. enzymes, transporters  
654 and regulators of anthocyanin biosynthesis for fruit color<sup>11,14,18</sup>, enzymes and regulators of wax and cutin  
655 biosynthesis pathways for glossiness and skin resistance<sup>59,61,63,64,67</sup>, and enzymes of primary metabolism,  
656 organic acid transporters and proton pumps for titratable acidity<sup>13,51,82,83,84</sup>. Their function in plant and fruit  
657 was then investigated by exploiting the Arabidopsis database (<https://www.arabidopsis.org/>) with  
658 corresponding TAIR accession numbers; the relevant literature, especially that relating to strawberry and  
659 other fleshy fruit species of the *Rosaceae* family; and gene expression patterns in strawberry fruit using *F.*  
660 *vesca* eFP browser<sup>85</sup>. For skin-associated traits, patterns of gene expression in plant organs and fruit cell  
661 types were further investigated in tomato, the fleshy fruit and cuticle model, using SGN-TEA  
662 (<https://tea.solgenomics.net/>) and Tomato eFP browser  
663 ([http://bar.utoronto.ca/efp2/Tomato/Tomato\\_eFPBrowser2.html](http://bar.utoronto.ca/efp2/Tomato/Tomato_eFPBrowser2.html)).

664

### 665 **Conflict of interest statement**

666 The authors declare that there are no conflicts of interest.

667

## 668 **Author's contributions**

669 BD and AIP conceived and designed the experiments. AIP conducted hands-on experiments and data  
670 collection. AuP, JoP and JuP contributed to data collection. AIP, PRS, BD and CR analyzed the data. AIP, BD  
671 and CR wrote the original draft. All authors read and approved the final manuscript.

672

## 673 **Acknowledgements**

674 We thank Sarah Touzani and Eva Bouillon for their help in phenotyping. The project was funded by the  
675 Nouvelle-Aquitaine Region and the European Regional Development Fund (ERDF) (REGINA project no.  
676 67822110; AgirClim project No. 2018-1R20202); and European Union Horizon 2020 research and innovation  
677 program (BreedingValue project No. 101000747; PRIMA-Partnership 2019-2022 Med-Berry project). AIP  
678 was supported by the CIFRE (Convention Industrielle de Formation par la Recherche) contract between  
679 Invenio (SME, Bordeaux, France) and the INRAE BAP department.

680

## 681 **Data availability**

682 All relevant data generated or analyzed are included in the manuscript and the supporting materials.

683

## 684 **References**

685

- 686 1. Edger PP, Poorten TJ, VanBuren R, et al. Origin and evolution of the octoploid strawberry genome. *Nat*  
687 *Genet.* 2019;51(3):541-547. doi:10.1038/s41588-019-0356-4
- 688 2. Whitaker VM, Knapp SJ, Hardigan MA, et al. A roadmap for research in octoploid strawberry. *Hortic*  
689 *Res.* 2020;7:33. doi:10.1038/s41438-020-0252-1
- 690 3. Pincot DDA, Ledda M, Feldmann MJ, et al. Social network analysis of the genealogy of strawberry:  
691 retracing the wild roots of heirloom and modern cultivars. *G3 (Bethesda)*. 2021;11(3):jkab015.  
692 doi:10.1093/g3journal/jkab015
- 693 4. Hardigan MA, Lorant A, Pincot DDA, et al. Unraveling the Complex Hybrid Ancestry and Domestication  
694 History of Cultivated Strawberry. *Mol Biol Evol.* 2021b;38(6):2285-2305. doi:10.1093/molbev/msab024
- 695 5. Feldmann MJ, Pincot DDA, Cole GS, Knapp SJ. Genetic gains underpinning a little-known strawberry  
696 Green Revolution. *Nat Commun.* 2024;15(1):2468. Published 2024 Mar 19. doi:10.1038/s41467-024-  
697 46421-6
- 698 6. Senger E, Osorio S, Olbricht K, et al. Towards smart and sustainable development of modern berry  
699 cultivars in Europe. *Plant J.* 2022;111(5):1238-1251. doi:10.1111/tpj.15876
- 700 7. Liu Z, Liang T, Kang C. Molecular bases of strawberry fruit quality traits: advances, challenges, and  
701 opportunities. *Plant Physiol.* 2023;kiad376. doi:10.1093/plphys/kiad376



- 702 8. Castillejo, C. et al. Allelic Variation of MYB10 is the Major Force Controlling Natural Variation of Skin  
703 and Flesh Color in Strawberry (*Fragaria* spp.) fruit. *Plant Cell* 32, 3723-3749 (2020).  
704 <https://doi.org/10.1105/tpc.20.00474>
- 705 9. Fan Z, Tieman DM, Knapp SJ, et al. A multi-omics framework reveals strawberry flavor genes and their  
706 regulatory elements. *New Phytol.* 2022;236(3):1089-1107. doi:10.1111/nph.18416
- 707 10. Lara I, Belge B, Goulao LF. A focus on the biosynthesis and composition of cuticle in fruits. *J Agric Food*  
708 *Chem.* 2015;63(16):4005-4019. doi:10.1021/acs.jafc.5b00013
- 709 11. Denoyes B, Prohaska A, Petit J, Rothan C. Deciphering the genetic architecture of fruit color in  
710 strawberry. *J Exp Bot.* 2023;erad245. doi:10.1093/jxb/erad245
- 711 12. Zorrilla-Fontanesi Y, Cabeza A, Domínguez P, et al. Quantitative trait loci and underlying candidate  
712 genes controlling agronomical and fruit quality traits in octoploid strawberry (*Fragaria* × *ananassa*).  
713 *Theor Appl Genet.* 2011;123(5):755-778. doi:10.1007/s00122-011-1624-6
- 714 13. Lerceteau-Köhler E, Moing A, Guérin G, et al. Genetic dissection of fruit quality traits in the octoploid  
715 cultivated strawberry highlights the role of homoeo-QTL in their control. *Theor Appl Genet.*  
716 2012;124(6):1059-1077. doi:10.1007/s00122-011-1769-3
- 717 14. Labadie M, Vallin G, Petit A, et al. Metabolite Quantitative Trait Loci for Flavonoids Provide New  
718 Insights into the Genetic Architecture of Strawberry (*Fragaria* × *ananassa*) Fruit Quality. *J Agric Food*  
719 *Chem.* 2020;68(25):6927-6939. doi:10.1021/acs.jafc.0c01855
- 720 15. Rey-Serra P, Mnejja M, Monfort A. Shape, firmness and fruit quality QTLs shared in two non-related  
721 strawberry populations. *Plant Sci.* 2021;311:111010. doi:10.1016/j.plantsci.2021.111010
- 722 16. Muñoz P, Castillejo C, Gómez JA, et al. QTL analysis for ascorbic acid content in strawberry fruit reveals  
723 a complex genetic architecture and association with GDP-L-galactose phosphorylase. *Hortic Res.*  
724 2023;10(3):uhad006. Published 2023 Jan 19. doi:10.1093/hr/uhad006
- 725 17. Cockerton HM, Karlström A, Johnson AW, et al. Genomic Informed Breeding Strategies for Strawberry  
726 Yield and Fruit Quality Traits. *Front Plant Sci.* 2021;12:724847. Published 2021 Oct 5.  
727 doi:10.3389/fpls.2021.724847
- 728 18. Labadie M, Vallin G, Potier A, et al. High Resolution Quantitative Trait Locus Mapping and Whole  
729 Genome Sequencing Enable the Design of an Anthocyanidin Reductase-Specific Homoeo-Allelic Marker  
730 for Fruit Colour Improvement in Octoploid Strawberry (*Fragaria* × *ananassa*). *Front Plant Sci.*  
731 2022;13:869655. doi:10.3389/fpls.2022.869655
- 732 19. Gaston A, Osorio S, Denoyes B, Rothan C. Applying the Solanaceae Strategies to Strawberry Crop  
733 Improvement. *Trends Plant Sci.* 2020;25(2):130-140. doi:10.1016/j.tplants.2019.10.003
- 734 20. Jin X, Du H, Zhu C, et al. Haplotype-resolved genomes of wild octoploid progenitors illuminate genomic  
735 diversifications from wild relatives to cultivated strawberry. *Nat Plants.* 2023;10.1038/s41477-023-  
736 01473-2. doi:10.1038/s41477-023-01473-2



- 737 21. Session AM, Rokhsar DS. Transposon signatures of allopolyploid genome evolution. *Nat Commun.*  
738 2023;14(1):3180. Published 2023 Jun 1. doi:10.1038/s41467-023-38560-z
- 739 22. Hardigan MA, Feldmann MJ, Lorant A, et al. Genome Synteny Has Been Conserved Among the  
740 Octoploid Progenitors of Cultivated Strawberry Over Millions of Years of Evolution. *Front Plant Sci.*  
741 2020;10:1789. doi:10.3389/fpls.2019.01789
- 742 23. Hardigan MA, Feldmann MJ, Pincot DDA, et al. Blueprint for Phasing and Assembling the Genomes of  
743 Heterozygous Polyploids: Application to the Octoploid Genome of Strawberry. *bioRxiv* 2021a; doi:  
744 10.1101/2021.11.03.467115. [Preprint].
- 745 24. Lee HE, Manivannan A, Lee SY, et al. Chromosome Level Assembly of Homozygous Inbred Line  
746 'Wongyo 3115' Facilitates the Construction of a High-Density Linkage Map and Identification of QTLs  
747 Associated With Fruit Firmness in Octoploid Strawberry (*Fragaria × ananassa*). *Front Plant Sci.*  
748 2021;12:696229. Published 2021 Jul 14. doi:10.3389/fpls.2021.696229
- 749 25. Han H, Barbey CR, Fan Z, Verma S, Whitaker VM, Lee S. Telomere-to-Telomere and Haplotype-Phased  
750 Genome Assemblies of the Heterozygous Octoploid 'Florida Brilliance' Strawberry (*Fragaria ×*  
751 *ananassa*). *bioRxiv* 2022.10.05.509768; doi: <https://doi.org/10.1101/2022.10.05.509768>.
- 752 26. Mao JX, Wang Y, Wang BT, Li JQ, Zhang C, Zhang WS, Li X, Li J, Zhang JX, Li H, Zhang ZH. High-quality  
753 haplotype-resolved genome assembly of cultivated octoploid strawberry. *Horticulture Research.*  
754 Volume 10, Issue 1, January 2023, uhad002, doi: 10.1093/hr/uhad002
- 755 27. Hummer K., Bassil NV., Zurn J., Amyotte B. Phenotypic characterization of a strawberry (*Fragaria*  
756 *xananassa* Duchesne ex Rosier) diversity collection. *Plants, People, Planet.* 2022;5(2):209-224.  
757 <https://doi.org/10.1002/ppp3.10316>
- 758 28. Zurn JD, Hummer KE, Bassil NV. Exploring the diversity and genetic structure of the U.S. National  
759 Cultivated Strawberry Collection. *Hortic Res.* 2022;9:uhac125. Published 2022 May 26.  
760 doi:10.1093/hr/uhac125
- 761 29. Fan Z, Whitaker VM. Genomic signatures of strawberry domestication and diversification. *Plant Cell.*  
762 Published online December 19, 2023. doi:10.1093/plcell/koad314
- 763 30. Oh Y, Barbey CR, Chandra S, et al. Genomic Characterization of the Fruity Aroma Gene, FaFAD1,  
764 Reveals a Gene Dosage Effect on  $\gamma$ -Decalactone Production in Strawberry (*Fragaria × ananassa*). *Front*  
765 *Plant Sci.* 2021;12:639345. doi:10.3389/fpls.2021.639345
- 766 31. Fan Z, Verma S, Lee H, Jang YJ, Wang Y, Lee S, Whitaker VM. Strawberry soluble solids QTL with inverse  
767 effects on yield. *Horticulture Research*, 2024; 11, uhad271, doi.org/10.1093/hr/uhad271
- 768 32. Horvath A, Sánchez-Sevilla JF, Punelli F, et al. Structured diversity in octoploid strawberry cultivars:  
769 importance of the old European germplasm. *Annals of Applied Biology* 2011;159(3): 358-371  
770 doi.org/10.1111/j.1744-7348.2011.00503.x

- 771 33. Edger PP, VanBuren R, Colle M, et al. Single-molecule sequencing and optical mapping yields an  
772 improved genome of woodland strawberry (*Fragaria vesca*) with chromosome-scale contiguity.  
773 *Gigascience*. 2018;7(2):1-7. doi:10.1093/gigascience/gix124
- 774 34. Sánchez-Sevilla JF, Horvath A, Botella MA, et al. Diversity Arrays Technology (DART) Marker Platforms  
775 for Diversity Analysis and Linkage Mapping in a Complex Crop, the Octoploid Cultivated Strawberry  
776 (*Fragaria* × *ananassa*). *PLoS One*. 2015;10(12):e0144960. Published 2015 Dec 16.  
777 doi:10.1371/journal.pone.0144960
- 778 35. Rosati P. Recent trends in strawberry production and research: an overview. *Acta Horticulturae*  
779 1993;348, 23–44. DOI:10.17660/ActaHortic.1993.348.1
- 780 36. Mezzetti, B., Giampieri, F., Zhang, Y.T. & Zhong, C.F. Status of strawberry breeding programs and  
781 cultivation systems in Europe and the rest of the world. *J. Berry Res*. 2018;8, 205-221.  
782 DOI:10.3233/JBR-180314
- 783 37. Davik J, Aaby K, Buti M, et al. Major-effect candidate genes identified in cultivated strawberry  
784 (*Fragaria* × *ananassa* Duch.) for ellagic acid deoxyhexoside and pelargonidin-3-O-malonylglucoside  
785 biosynthesis, key polyphenolic compounds. *Hortic Res*. 2020;7:125. Published 2020 Aug 1.  
786 doi:10.1038/s41438-020-00347-4
- 787 38. Nagamatsu S, Tsubone M, Wada T, et al. Strawberry fruit shape: quantification by image analysis and  
788 QTL detection by genome-wide association analysis. *Breed Sci*. 2021;71(2):167-175.  
789 doi:10.1270/jsbbs.19106
- 790 39. Muñoz P, Roldán-Guerra FJ, Verma S, Ruiz-Velázquez M, Torreblanca R, Oiza N, Castillejo C, Sánchez-  
791 Sevilla JF, Amaya I. Genome-wide association studies in a diverse strawberry collection unveil loci  
792 controlling agronomic and fruit quality traits. *bioRxiv* 2024;doi: 10.1101/2024.03.11.584394.  
793 [Preprint].
- 794 40. Alarfaj R, El-Soda M, Antanaviciute L, et al. Mapping QTL underlying fruit quality traits in an F1  
795 strawberry population. *The Journal of Horticultural Science and Biotechnology*. 2021;96(5), 634–645.  
796 <https://doi.org/10.1080/14620316.2021.1912647>
- 797 41. Natarajan S, Hossain MR, Kim HT, et al. ddRAD-seq derived genome-wide SNPs, high density linkage  
798 map and QTLs for fruit quality traits in strawberry (*Fragaria* × *ananassa*). *3 Biotech*. 2020;10(8):353.  
799 doi:10.1007/s13205-020-02291-5
- 800 42. Sieczko L, Masny A., Pruski K., Żurawicz E., Mądry W. Multivariate assessment of cultivars' biodiversity  
801 among the Polish strawberry core collection. *Hort. Sci. (Prague)*. 2015;42: 83–93. doi:  
802 10.17221/123/2014-HORTSCI
- 803 43. Lewers KS, Michael JN, Eunhee P, Yaguang L. Consumer preference and physiochemical analyses of  
804 fresh strawberries from ten cultivars. *International Journal of Fruit Science*. 2020;20:sup2, 733-756,  
805 DOI: 10.1080/15538362.2020.1768617

- 806 44. van der Knaap E, Chakrabarti M, Chu YH, et al. What lies beyond the eye: the molecular mechanisms  
807 regulating tomato fruit weight and shape. *Front Plant Sci.* 2014;5:227. Published 2014 May 27.  
808 doi:10.3389/fpls.2014.00227
- 809 45. Wu S, Zhang B, Keyhaninejad N, et al. A common genetic mechanism underlies morphological diversity  
810 in fruits and other plant organs. *Nat Commun.* 2018;9(1):4734. Published 2018 Nov 9.  
811 doi:10.1038/s41467-018-07216-8
- 812 46. Griesser M, Hoffmann T, Bellido ML, et al. Redirection of flavonoid biosynthesis through the down-  
813 regulation of an anthocyanidin glucosyltransferase in ripening strawberry fruit. *Plant Physiol.*  
814 2008;146(4):1528-1539. doi:10.1104/pp.107.114280
- 815 47. Marinova K, Pourcel L, Weder B, et al. The Arabidopsis MATE transporter TT12 acts as a vacuolar  
816 flavonoid/H<sup>+</sup> -antiporter active in proanthocyanidin-accumulating cells of the seed coat. *Plant Cell.*  
817 2007;19(6):2023-2038. doi:10.1105/tpc.106.046029
- 818 48. Moya-León MA, Mattus-Araya E, Herrera R. Molecular Events Occurring During Softening of  
819 Strawberry Fruit. *Front Plant Sci.* 2019;10:615. Published 2019 May 15. doi:10.3389/fpls.2019.00615
- 820 49. Jiménez-Bermúdez S, Redondo-Nevado J, Muñoz-Blanco J, et al. Manipulation of strawberry fruit  
821 softening by antisense expression of a pectate lyase gene. *Plant Physiol.* 2002;128(2):751-759.  
822 doi:10.1104/pp.010671
- 823 50. García-Gago JA, Posé S, Muñoz-Blanco J, Quesada MA, Mercado JA. The polygalacturonase FaPG1 gene  
824 plays a key role in strawberry fruit softening. *Plant Signal Behav.* 2009;4(8):766-768.  
825 doi:10.1104/pp.109.138297
- 826 51. Moing, A., Renaud, C., Gaudillère, M., Raymond, P., Roudeillac, P., & Denoyes-Rothan, B. Biochemical  
827 Changes during Fruit Development of Four Strawberry Cultivars. *Journal of the American Society for*  
828 *Horticultural Science* jashs 2001;126(4), 394-403. <https://doi.org/10.21273/JASHS.126.4.394>
- 829 52. Ruan YL. Sucrose metabolism: gateway to diverse carbon use and sugar signaling. *Annu Rev Plant Biol.*  
830 2014;65:33-67. doi:10.1146/annurev-arplant-050213-040251
- 831 53. Miron D, Petreikov M, Carmi N, et al. Sucrose uptake, invertase localization and gene expression in  
832 developing fruit of *Lycopersicon esculentum* and the sucrose-accumulating *Lycopersicon hirsutum*.  
833 *Physiol Plant.* 2002;115(1):35-47. doi:10.1034/j.1399-3054.2002.1150104.x
- 834 54. Fridman E, Carrari F, Liu YS, Fernie AR, Zamir D. Zooming in on a quantitative trait for tomato yield  
835 using interspecific introgressions. *Science.* 2004;305(5691):1786-1789. doi:10.1126/science.1101666
- 836 55. Afoufa-Bastien D, Medici A, Jeauffre J, et al. The *Vitis vinifera* sugar transporter gene family:  
837 phylogenetic overview and macroarray expression profiling. *BMC Plant Biol.* 2010;10:245. Published  
838 2010 Nov 12. doi:10.1186/1471-2229-10-245.

- 839 56. Yang M, Hou G, Peng Y, et al. FaGAPC2/FaPKc2.2 and FaPEPCK reveal differential citric acid metabolism  
840 regulation in late development of strawberry fruit. *Front Plant Sci.* 2023;14:1138865. Published 2023  
841 Apr 4. doi:10.3389/fpls.2023.1138865
- 842 57. Shlizerman L, Marsh K, Blumwald E, Sadka A. Iron-shortage-induced increase in citric acid content and  
843 reduction of cytosolic aconitase activity in Citrus fruit vesicles and calli. *Physiol Plant.* 2007;131(1):72-  
844 79. doi:10.1111/j.1399-3054.2007.00935.x
- 845 58. Huang XY, Wang CK, Zhao YW, Sun CH, Hu DG. Mechanisms and regulation of organic acid  
846 accumulation in plant vacuoles. *Hortic Res.* 2021;8(1):227. Published 2021 Oct 25.  
847 doi:10.1038/s41438-021-00702-z
- 848 59. Reynoud N, Petit J, Bres C, et al. The Complex Architecture of Plant Cuticles and Its Relation to Multiple  
849 Biological Functions. *Front Plant Sci.* 2021;12:782773. Published 2021 Dec 10.  
850 doi:10.3389/fpls.2021.782773
- 851 60. Bargel H, Neinhuis C. Tomato (*Lycopersicon esculentum* Mill.) fruit growth and ripening as related to  
852 the biomechanical properties of fruit skin and isolated cuticle. *J Exp Bot.* 2005;56(413):1049-1060.  
853 doi:10.1093/jxb/eri098
- 854 61. Petit J, Bres C, Mauxion JP, Bakan B, Rothan C. Breeding for cuticle-associated traits in crop species:  
855 traits, targets, and strategies. *J Exp Bot.* 2017;68(19):5369-5387. doi:10.1093/jxb/erx341!
- 856 62. Järvinen R, Kaimainen M, Kallio H. Cutin composition of selected northern berries and seeds, *Food*  
857 *Chemistry.* 2010;Volume 122, Issue 1, pages 137-144.  
858 <https://doi.org/10.1016/j.foodchem.2010.02.030>
- 859 63. Petit J, Bres C, Just D, et al. Analyses of tomato fruit brightness mutants uncover both cutin-deficient  
860 and cutin-abundant mutants and a new hypomorphic allele of GDSL lipase. *Plant Physiol.*  
861 2014;164(2):888-906. doi:10.1104/pp.113.232645
- 862 64. Petit J, Bres C, Mauxion JP, et al. The Glycerol-3-Phosphate Acyltransferase GPAT6 from Tomato Plays a  
863 Central Role in Fruit Cutin Biosynthesis. *Plant Physiol.* 2016;171(2):894-913. doi:10.1104/pp.16.00409
- 864 65. Liu Q, Huang H, Chen Y, et al. Two Arabidopsis MYB-SHAQKYF transcription repressors regulate leaf  
865 wax biosynthesis via transcriptional suppression on DEWAX. *New Phytol.* 2022;236(6):2115-2130.  
866 doi:10.1111/nph.18498
- 867 66. Kriegshauser L, Knosp S, Grienberger E, et al. Function of the HYDROXYCINNAMOYL-CoA:SHIKIMATE  
868 HYDROXYCINNAMOYL TRANSFERASE is evolutionarily conserved in embryophytes. *Plant Cell.*  
869 2021;33(5):1472-1491. doi:10.1093/plcell/koab044
- 870 67. Girard AL, Mounet F, Lemaire-Chamley M, et al. Tomato GDSL1 is required for cutin deposition in the  
871 fruit cuticle. *Plant Cell.* 2012;24(7):3119-3134. doi:10.1105/tpc.112.101055

- 872 68. Ursache R, De Jesus Vieira Teixeira C, Déneraud Tendon V, et al. GDSL-domain proteins have key roles  
873 in suberin polymerization and degradation. *Nat Plants*. 2021;7(3):353-364. doi:10.1038/s41477-021-  
874 00862-9
- 875 69. Li R, Sun S, Wang H, et al. FIS1 encodes a GA2-oxidase that regulates fruit firmness in tomato. *Nat*  
876 *Commun*. 2020;11(1):5844. Published 2020 Nov 17. doi:10.1038/s41467-020-19705-w
- 877 70. Ma Y, Shafee T, Mudiyansele AM, et al. Distinct functions of FASCILIN-LIKE ARABINO GALACTAN  
878 PROTEINS relate to domain structure [published correction appears in *Plant Physiol*. 2023 Aug  
879 3;192(4):3203]. *Plant Physiol*. 2023;192(1):119-132. doi:10.1093/plphys/kiad097
- 880 71. Bates D, Mächler M, Bolker B, Walker S. Fitting Linear Mixed-Effects Models Using lme4. *Journal of*  
881 *Statistical Software*. 2015;67:1–48. DOI:10.18637/jss.v067.i01
- 882 72. Pritchard JK, Stephens M, Donnelly P. Inference of Population Structure Using Multilocus Genotype  
883 Data, *Genetics*. 2000;155: 945–959. <https://doi.org/10.1093/genetics/155.2.945>.
- 884 73. Earl, Dent A. and vonHoldt, Bridgett M. STRUCTURE HARVESTER: a website and program for visualizing  
885 STRUCTURE output and implementing the Evanno method. *Conservation Genetics Resources*  
886 2011;DOI: 10.1007/s12686-011-9548-7
- 887 74. Wickham H ggplot2: Elegant Graphics for Data Analysis. Springer-Verlag New York. 2016;ISBN 978-3-  
888 319-24277-4. <https://ggplot2.tidyverse.org>.
- 889 75. Lê S, Josse J, Husson F. FactoMineR: A Package for Multivariate Analysis. *Journal of Statistical Software*.  
890 2008;25(1), 1–18. doi:10.18637/jss.v025.i01
- 891 76. Minh BQ, Schmidt HA, Chernomor O, et al. IQ-TREE 2: New Models and Efficient Methods for  
892 Phylogenetic Inference in the Genomic Era [published correction appears in *Mol Biol Evol*. 2020 Aug  
893 1;37(8):2461]. *Mol Biol Evol*. 2020;37(5):1530-1534. doi:10.1093/molbev/msaa015
- 894 77. Mangin B, Siberchicot A, Nicolas S, Doligez A, This P, Cierco-Ayrolles C. Novel measures of linkage  
895 disequilibrium that correct the bias due to population structure and relatedness. *Heredity (Edinb)*.  
896 2012;108(3):285-291. doi:10.1038/hdy.2011.73
- 897 78. Bradbury PJ, Zhang Z, Kroon DE, Casstevens TM, Ramdoss Y, Buckler ES. TASSEL: software for  
898 association mapping of complex traits in diverse samples. *Bioinformatics*. 2007;23(19):2633-2635.  
899 doi:10.1093/bioinformatics/btm308
- 900 79. Luu K, Bazin E, Blum MG. pcadapt: an R package to perform genome scans for selection based on  
901 principal component analysis. *Mol Ecol Resour*. 2017;17(1):67-77. doi:10.1111/1755-0998.12592
- 902 80. Wang J, Zhang Z. GAPIT Version 3: Boosting Power and Accuracy for Genomic Association and  
903 Prediction. *Genomics Proteomics Bioinformatics*. 2021 Aug;19(4):629-640. doi:  
904 10.1016/j.gpb.2021.08.005. Epub 2021 Sep 4. PMID: 34492338; PMCID: PMC9121400.

- 905 81. Huang M, Liu X, Zhou Y, Summers RM, Zhang Z. BLINK: a package for the next level of genome-wide  
906 association studies with both individuals and markers in the millions. *Gigascience*. 2019 Feb  
907 1;8(2):giy154. doi: 10.1093/gigascience/giy154. PMID: 30535326; PMCID: PMC6365300.
- 908 82. Causse M, Duffe P, Gomez MC, et al. A genetic map of candidate genes and QTLs involved in tomato  
909 fruit size and composition. *J Exp Bot*. 2004;55(403):1671-1685. doi:10.1093/jxb/erh207
- 910 83. Etienne C, Rothan C, Moing A, et al. Candidate genes and QTLs for sugar and organic acid content in  
911 peach [ *Prunus persica* (L.) Batsch]. *Theor Appl Genet*. 2002;105(1):145-159. doi:10.1007/s00122-001-  
912 0841-9
- 913 84. Etienne C, Moing A, Dirlewanger E, Raymond P, Monet R, Rothan C. Isolation and characterization of  
914 six peach cDNAs encoding key proteins in organic acid metabolism and solute accumulation:  
915 involvement in regulating peach fruit acidity. *Physiol Plant*. 2002;114(2):259-270. doi:10.1034/j.1399-  
916 3054.2002.1140212.x
- 917 85. Hawkins C, Caruana J, Li J, et al. An eFP browser for visualizing strawberry fruit and flower  
918 transcriptomes. *Hortic Res*. 2017;4:17029. Published 2017 Jun 21. doi:10.1038/hortres.2017.29
- 919  
920  
921